

DOUBLED DISKS AND SATELLITE SURFACES

GARY GUTH, KYLE HAYDEN, SUNGKYUNG KANG, AND JUNGHWAN PARK

ABSTRACT. Conjecturally, a knot is slice if and only if its positive Whitehead double is slice. We consider an analogue of this conjecture for slice disks in the four-ball: two slice disks of a knot are smoothly isotopic if and only if their positive Whitehead doubles are smoothly isotopic. We provide evidence for this conjecture, using a range of techniques. More generally, we consider when isotopy obstructions persist under satellite operations. In particular, we show that obstructions coming from knot Floer homology, Seiberg-Witten theory, and Khovanov homology often behave well under satellite operations.

We apply these strategies to give a systematic method for constructing vast numbers of exotic disks in the four-ball, including the first infinite family of pairwise exotic slice disks. These same techniques are then upgraded to produce exotic disks that remain exotic after any prescribed number of internal stabilizations. Finally, we show that the branched double covers of certain stably-exotic disks become diffeomorphic after a single stabilization with $S^2 \times S^2$, hence stabilizing them yields exotic surfaces that have diffeomorphic branched covers.

1. INTRODUCTION

Given a knot K in the 3-sphere and a pattern knot P embedded in the solid torus, the *satellite of K with pattern P* is defined by cutting out a neighborhood of K and filling it with the solid torus containing P . We will denote the resulting knot $P(K)$.

Satellite operations are ubiquitous in the study of knots in dimension three, but also have natural four dimensional extensions. Given a concordance C from K_0 to K_1 , there is satellite concordance from $P(K_0)$ to $P(K_1)$, denoted $P(C)$, which is obtained by cutting out a neighborhood of the concordance and gluing back in the pattern cylinder $(S^1 \times D^1 \times [0, 1], P \times [0, 1])$. When K_0 is the unknot and the pattern P is unknotted, the satellite construction uniquely determines a satellite slice disk for $P(K_1)$; see Figure 1.1 for examples. These ideas extend further to higher-genus surfaces and surfaces in other 4-manifolds (e.g., [Shi71, HKK⁺21, HKM⁺22]).

The question of how knot invariants behave under satellite operations is well-studied. We aim to further the analogous study of the behavior of surface invariants under satellite operations, and tease out some of the similarities in the two contexts. We conjecture that many satellite operations are “injective”; we show, that for large families of satellite patterns, disks which can be smoothly distinguished often have satellite disks which are also smoothly distinguishable. Matters are quite different in the topological category: by the work of Conway and Powell [CP21b], under suitable satellite operations, disks which were initially topologically distinct can become topologically isotopic. This stark contrast leads us to consider the ways in which satellite operations can be used in the study of exotic phenomena.

In particular, we see that satellite operations can help address a fundamental dilemma: finding constructions that are mild enough to preserve the topological type of an object

GG is partially supported by NSF Grant DMS-2204214 and a Simons Collaboration Grant on New Structures in Low Dimensional Topology. KH is supported by NSF grant DMS-2243128. JP is partially supported by Samsung Science and Technology Foundation (SSTF-BA2102-02) and the POSCO TJ Park Science Fellowship.

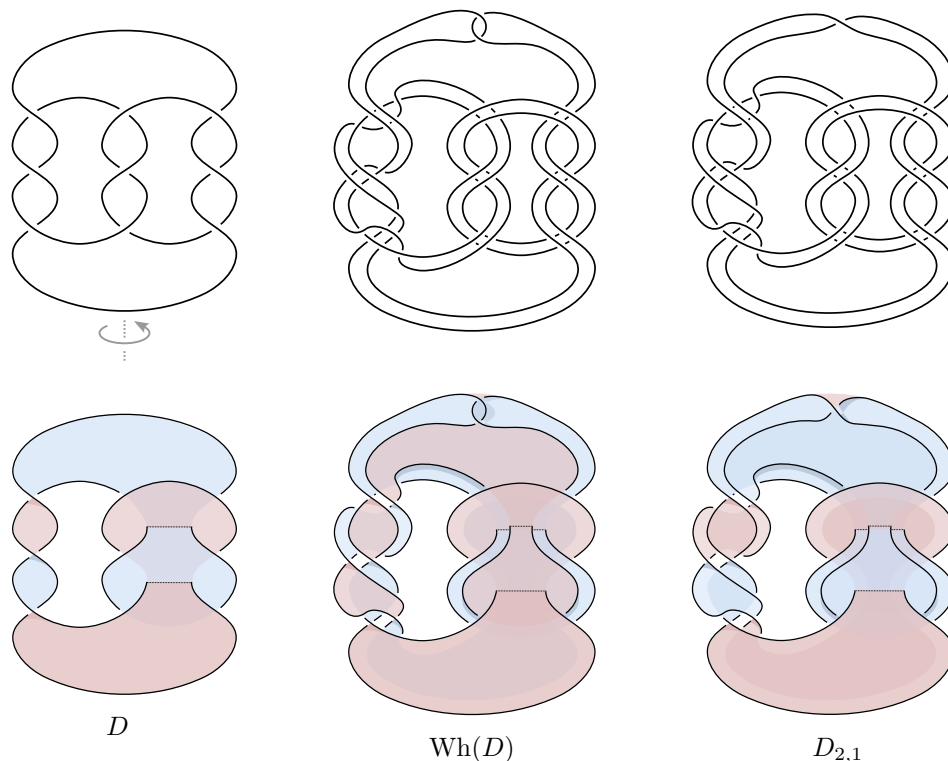


FIGURE 1.1. A slice disk for $m(9_{46})$, together with its Whitehead double and $(2,1)$ -cable.

yet are significant enough to cause a measurable change in its smooth type. For example, Fintushel and Stern's *rim surgery* operation [FS97] aims to strike this balance directly, and variations of this operation have led to virtually all known examples of infinite families of exotic surfaces. An alternative is to begin with a violent operation that changes both the smooth *and* topological type, and then apply a second operation (e.g., Whitehead doubling) to erase the topological difference between the surfaces.

In this paper, we study slice disks that are *exotically knotted* (i.e., topologically isotopic rel boundary but not smoothly isotopic rel boundary) using three different techniques: knot Floer homology, Khovanov homology, and Seiberg-Witten invariants. We briefly outline their strengths and weaknesses here. Knot Floer homology supports the most broadly applicable techniques among the three, and indeed it produces the most general statements in this paper thanks to tools coming from bordered Floer homology [LOT18]. In contrast, making general statements about surface invariants in Khovanov homology is quite difficult, especially given its lack of analogous bordered techniques. However, it has the advantage of being inherently combinatorial, which allows us to make simple computations. Finally, we make essential use of the fact that the Seiberg-Witten invariants are defined over \mathbb{Z} coefficients; this allows us to distinguish infinite families of pairwise exotic disks bounded by the same knot.

1.1. Satellite Operators. By the work of Freedman [Fre82, FQ90], any knot in S^3 with trivial Alexander polynomial is topologically slice. The Alexander polynomial behaves well with respect to satellite operations: if $P(K)$ is a satellite knot with pattern P and

companion K , the Alexander polynomial of $P(K)$ can be computed as

$$\Delta_{P(K)}(t) = \Delta_P(t) \cdot \Delta_K(t^w),$$

where the pattern P represents w times the generator for $H_1(S^1 \times D^2)$. As a consequence, the positive Whitehead double of a knot K is always topologically slice. This contrasts with the smooth setting, where the following remains a major open problem:

Conjecture 1.1 ([Kir78, Problem 1.38]). *A knot K is smoothly slice if and only if its positive Whitehead double is smoothly slice.*

In [Hed07], Hedden provided strong evidence for this conjecture by showing that if $\tau(K) > 0$ then $\tau(\text{Wh}(K))$ is nonzero. In particular, if knot Floer homology obstructs K from being smoothly slice it will obstruct $\text{Wh}(K)$ from being smoothly slice as well.

Inspired by the situation in three dimensions, we consider the analogous case of slice disks in the four-ball. Conway and Powell [CP21a] showed that if D_1 and D_2 are slice disks for a knot K , then they are topologically isotopic if

$$\pi_1(B^4 \setminus \nu D_1) \cong \mathbb{Z} \cong \pi_1(B^4 \setminus \nu D_2).$$

As a consequence, the positive Whitehead doubles of any two slice disks for a knot K are topologically isotopic (see Section 2). Given Conjecture 1.1, it is natural to ask whether the smooth isotopy class of a slice disk is determined by that of its Whitehead double.

Conjecture 1.2. *Two slice disks for a knot K are smoothly isotopic if and only if their positive Whitehead doubles are smoothly isotopic.*

In Section 4, we prove an analogue of [Hed07, Corollary 1.5] showing that if a pair of slice disks are distinguished by knot Floer homology then their positive Whitehead doubles will be distinguished as well. Given a slice disk D of K , we denote the induced element $F_D(1)$ in $\widehat{HFK}(S^3, K)$ by t_D .

Theorem A. *Let K be a knot in S^3 with slice disks D_1 and D_2 . If $t_{D_1} \neq t_{D_2}$, then $t_{\text{Wh}(D_1)} \neq t_{\text{Wh}(D_2)}$ as well.*

In fact, we prove an analogous result for many satellite operations, including positive $(p, 1)$ -cables (Theorem B), the Mazur pattern (Example 4.4), and a large class of satellite patterns introduced by Levine [Lev12] that generalizes Whitehead doubling (Proposition 4.1). Our proof relies on an analysis of the type A module associated to the pattern knot embedded in the solid torus. In particular, our proof holds for any unknotted pattern satisfying a technical condition on the type A structure, which we expect to hold for many unknotted patterns.

Our corresponding result for cabling patterns shows that $(p, 1)$ -cabling does more than preserve the difference between disks distinguished by knot Floer homology — it increases the distance between them. To state this precisely, we recall the operation of (*internal*) *stabilization* of a knotted surface as described in [BS16, §2.1]: given an embedded surface $S \subset B^4$, choose an embedded 3-dimensional 1-handle $h \approx [-1, 1] \times D^2$ in B^4 that intersects S only along $\{\pm 1\} \times D^2$, then increase the genus of S by removing $\{\pm 1\} \times D^2$ from S and gluing in $[-1, 1] \times D^2$. We show that the $(p, 1)$ -cables of disks which are distinguished by knot Floer homology must always have stabilization distance at least p .

Theorem B. *Let K be a knot in S^3 with slice disks D_1 and D_2 . If $t_{D_1} \neq t_{D_2}$, then for any integer $p \geq 1$, we have $t_{(D_1)_{p,1}} \neq t_{(D_2)_{p,1}}$. Furthermore, the stabilization distance between $(D_1)_{p,1}$ and $(D_2)_{p,1}$ is at least p .*

Below, we describe applications of these results and related techniques to the study of exotic surfaces.

1.2. Exotically knotted surfaces. While the results above show that smoothly distinct disks often remain distinct under various satellite operations, things are quite different in the topological category. Applying the work of Conway and Powell [CP21b, Theorem 1.2], we show that for any unknotted, winding number zero pattern P and any pair of disks $D_1, D_2 \subset B^4$ with the same boundary, the satellite disks $P(D_1)$ and $P(D_2)$ are topologically isotopic rel boundary. In particular, given any pair of slice disks for a knot $K \subset S^3$, their Whitehead doubles are always topologically isotopic. Therefore, the obstructive results from Section 1.1 imply the existence of vast numbers of exotic disks; by starting with disks which can be distinguished by knot Floer homology we can produce an exotic pair by applying the Whitehead doubling operator.

Corollary A.1. *Let K be a knot in S^3 with slice disks D_1 and D_2 . If $t_{D_1} \neq t_{D_2}$, then $\text{Wh}(D_1)$ and $\text{Wh}(D_2)$ are exotically knotted.*

For example, we show that any nontrivial knot of the form $K \# K \# -K \# -K$ (which we will write as $2K \# -2K$) has a pair of slice disks distinguished by knot Floer homology, implying the following:

Corollary A.2. *If K is a nontrivial knot, then the knot $\text{Wh}(2K \# -2K)$ bounds an exotic pair of disks.*

Recall that disks are called *n-stably exotic* if they remain exotic after applying n internal stabilizations. Combining Theorem B with Corollary A.2 yields many n -stably exotic pairs for arbitrarily large values of n , significantly expanding on the results of [Gut22].

As another example, we consider the infinite family of slice disks for $4_1 \# 4_1$ obtained by roll-spinning [Fox66] (see also Figure 5.1); these are distinct up to topological isotopy rel boundary (e.g., by comparing their *peripheral maps* [JZ20, §3]). In [JZ21], Juhász and Zemke show that knot Floer homology is able to distinguish the first two members of this family of disks (up to smooth isotopy rel boundary), hence their Whitehead doubles are exotic by Corollary A.1. However, in its current state, knot Floer homology cannot distinguish all members of this infinite family of disks. This would require naturality and functoriality of the link cobordism maps for integral coefficients as well as a formula for the basepoint moving action with integral coefficients [Sar15, Zem16]. Nevertheless, we are able to distinguish the entire family of slice disks for $\text{Wh}(4_1 \# 4_1)$ indirectly using Seiberg-Witten invariants, building on arguments of Gompf [Gom17a, Gom17b] and Akbulut [Akb17].

Theorem C. *The knot $\text{Wh}(4_1 \# 4_1)$ bounds an infinite family of pairwise exotic slice disks.*

Applying techniques of Akbulut and Ruberman [AR16, Rub90], we can upgrade the examples in Theorem C to drop the “rel boundary” condition and produce an infinite collection of exotic slice disks that are *absolutely exotic*, i.e., not related by any smooth isotopy of B^4 .

Corollary C.1. *There exists a knot in S^3 that bounds an infinite family of exotic slice disks in B^4 that are not related by any smooth isotopy of B^4 .*

There is a close connection between exotically knotted surfaces and exotic 4-manifolds, especially through branched covering and surgery operations. For example, Finashin-Kreck-Viro constructed the first examples of exotically unknotted (nonorientable) closed surfaces in S^4 by proving that their branched double covers are exotic [FKV87]. Furthermore, it has been hoped that an exotic S^4 might be realized through surgery, i.e. Gluck twist [Glu62], or taking a branched cover, along knotted 2-spheres in S^4 . By taking branched covers of exotic surfaces that remain distinct after internal stabilization with T^2 (such as those in [Gut22]),

one obtains natural candidates for exotic 4-manifolds that remain distinct after an external stabilization with $S^2 \times S^2$ (c.f., [BS16]). However, we show that the branched covers of many stably exotic surfaces fail to yield stably exotic 4-manifolds:

Theorem D. *There are surfaces $S, S' \subset B^4$ that are exotically knotted (rel boundary) yet whose branched double covers $\Sigma_2(B^4, S)$ and $\Sigma_2(B^4, S')$ are diffeomorphic (rel boundary). Moreover, we may construct $S, S' \subset B^4$ by internally stabilizing a pair of exotic slice disks $D, D' \subset B^4$ whose branched double covers $\Sigma_2(B^4, D)$ and $\Sigma_2(B^4, D')$ are exotic (rel boundary).*

Experts may notice that the surfaces in our proof of Theorem D are precisely those arising in [Gut22], which constituted the first known examples of stably exotic slice disks.

1.3. Khovanov homology. Several recent results have employed the cobordism maps on Khovanov homology to detect exotically knotted surfaces in B^4 [HS21, HKM⁺22, Hay23, LS22]. In some contexts, the combinatorial nature of these invariants make their calculation more accessible than for their Floer-theoretic counterparts, and they appear to be better-suited to surfaces of higher genus (including those of non-minimal genus [HKM⁺22]). Although Khovanov homology lacks the well-developed bordered theory of Heegaard Floer homology, some recent results have shed light on the effect of certain satellite operations on Rasmussen's invariant [LZ22] (see also [Zib22]) and the Khovanov cobordism maps [HKM⁺22], including distinguishing Whitehead doubles of certain Seifert surfaces. Here we extend the latter approach to the study of slice disks. Although we do not prove a general result analogous to Theorems A and B for Khovanov homology, it can be shown that in many cases, the existence of cycles in Khovanov homology that distinguish a pair of slice disks can often be used to find cycles that distinguish satellites of those disks. We illustrate this with the following result.

Proposition E. *The knot $m(9_{46})$ bounds a pair of slice disks $D, D' \subset B^4$ whose Whitehead doubles $\text{Wh}(D), \text{Wh}(D')$ and $(2, 1)$ -cables $D_{2,1}, D'_{2,1}$ are distinguished by their maps on Khovanov homology, $\text{Kh}(\text{Wh}(D)) \neq \text{Kh}(\text{Wh}(D'))$ and $\text{Kh}(D_{2,1}) \neq \text{Kh}(D'_{2,1})$. Moreover, the maps $\text{BN}(D_{2,1})$ and $\text{BN}(D'_{2,1})$ on Bar-Natan homology over $\mathbb{F}_2[U]$ remain distinct after multiplication by U , hence these disks induce distinct maps after one internal stabilization.*

It seems possible that further study of satellite operations on Khovanov homology and Bar-Natan homology may yield results analogous to Theorems A and B.

1.4. Conventions. Throughout this paper, the unknot will be denoted by U . The satellite of a knot K with pattern P will be written as $P(K)$. The notation $\nu(\cdot)$ will be used to denote an open tubular neighborhood, and $\bar{\nu}(\cdot)$ its closure. Isotopies of disks are always taken to be fixed on the boundary unless otherwise specified.

2. PRELIMINARIES

In this section, we review the construction of satellite disks and establish a class of satellite patterns which are guaranteed to produce \mathbb{Z} -disks.

2.1. Satellite disks. Given a pattern P with $P(U) = U$ and a slice disk D which bounds a knot K , define the *satellite disk* $P(D)$ as follows. Let B be a neighborhood of a point in D . Then $D_0 := D \setminus B$ is a concordance in $B^4 \setminus B \cong S^3 \times I$ between U and K . We can then apply the pattern P , which gives a concordance $P(D_0)$ between $P(U) = U$ and $P(K)$. By capping off $P(U) = U$ with the trivial slice disk for the unknot, we obtain the satellite disk $P(D)$ for K .

A slice disk D is called a \mathbb{Z} -disk if the fundamental group of its complement is isomorphic to \mathbb{Z} . By the work of Conway and Powell, any two \mathbb{Z} -disks with common boundary are topologically isotopic rel. boundary [CP21a, Theorem 1.2]. We can arrange to work in this situation by choosing appropriate satellite patterns. Recall that the *winding number* of a pattern P is the algebraic intersection of P with a generic meridional disk of the solid torus containing P .

Proposition 2.1. *If P is a winding number zero pattern with $P(U) = U$ and D is a slice disk, then the satellite disk $P(D)$ is a \mathbb{Z} -disk.*

Proof. Choose a tubular neighborhood νD of D . The satellite disk $P(D)$ is contained in νD , so we have a splitting

$$B^4 \setminus P(D) = (B^4 \setminus \nu D) \cup (\bar{\nu} D \setminus P(D)).$$

Since homeomorphism class of $\bar{\nu} D \setminus P(D)$ does not depend on the choice of D ,

$$\bar{\nu} D \setminus P(D) \cong \bar{\nu}(D_0) \setminus P(D_0),$$

where D_0 denotes the trivial slice disk of an unknot U . It is clear that $P(D_0)$ is also a trivial slice disk of $P(U) = U$ and we may take $\bar{\nu}(D_0)$ to be the whole B^4 . Therefore,

$$\bar{\nu}(D_0) \setminus P(D_0) \cong B^4 \setminus D_0 \cong D^2 \times (D^2 \setminus \{pt\}),$$

implying $\pi_1(\nu D \setminus P(D)) \cong \mathbb{Z}$.

The fundamental group of the intersection

$$(B^4 \setminus \nu D) \cap (\bar{\nu} D \setminus P(D)) \cong S^1 \times D,$$

is clearly also \mathbb{Z} , and the natural maps

$$\begin{aligned} \pi_1((B^4 \setminus \nu D) \cap (\bar{\nu} D \setminus P(D))) &\rightarrow \pi_1(B^4 \setminus \nu D), \\ \pi_1((B^4 \setminus \nu D) \cap (\bar{\nu} D \setminus P(D))) &\rightarrow \pi_1(\nu D \setminus P(D)), \end{aligned}$$

are given by the inclusion of a meridional class of $\pi_1(B^4 \setminus \nu D)$ and the multiplication map $\mathbb{Z} \xrightarrow{\times w(P)} \mathbb{Z}$, respectively, where $w(P)$ denotes the winding number of P . Since P has winding number 0 and $\pi_1(B^4 \setminus \nu D)$ is normally generated by a meridian of D , we see

$$\pi_1(B^4 \setminus P(D)) \cong \pi_1(\bar{\nu} D \setminus P(D)) \cong \mathbb{Z}.$$

Therefore $P(D)$ is a \mathbb{Z} -disk. □

Example 2.2. Let D denote the slice disk for $m(9_{46})$ from Figure 1.1 and let D' be obtained by applying the involution shown in the top left of Figure 1.1. By Proposition 2.1, the Whitehead doubled disks $\text{Wh}(D)$ and $\text{Wh}(D')$ are \mathbb{Z} -disks with the same boundary $\text{Wh}(m(9_{46}))$, hence they are topologically isotopic rel. boundary by [CP21a, Theorem 1.2]. In later sections we will prove that these disks are *not* smoothly isotopic rel. boundary.

Knot doubling (which we now describe) produces an infinite family of patterns which satisfy the assumptions of Proposition 2.1. Given a knot J and an integer s , the doubling pattern $P_{J,s}$ is shown in Figure 2.1; the box labeled J, s represents s -framed parallel copies of $J \setminus \{pt\}$. This operation generalizes Whitehead doubling, which is recovered by taking J to be the unknot and $s = \pm 1$. These satellites are described more carefully as twisted infections along components of the Borromean rings in [Lev12, Section 1]. Since these patterns are unknotted, for any slice disk D , the doubled disk $P_{J,s}(D)$ is a \mathbb{Z} -disk. Moreover, by the formula for the Alexander polynomial of a satellite knot, the knot $P_{J,s}(K)$ is an Alexander polynomial 1 knot.

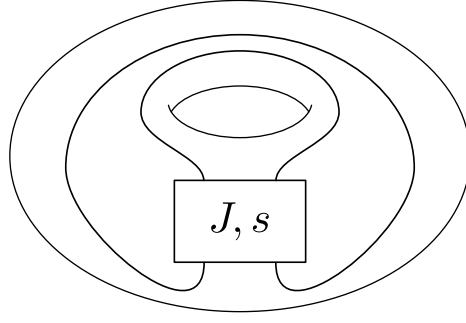


FIGURE 2.1. The doubling pattern associated to a knot J with framing s .

It is worth observing here that, in contrast with Proposition 2.1, patterns with nonzero winding number preserve most of the information about the fundamental group of a slice disk's complement.

Proposition 2.3. *Let P be a pattern with nonzero winding number.*

- (a) *For any knot $K \subset S^3$, the inclusion-induced map $\pi_1(S^3 \setminus K) \cong \pi_1(S^3 \setminus \nu K) \rightarrow \pi_1(S^3 \setminus P(K))$ is injective.*
- (b) *For any slice disk $D \subset B^4$, the inclusion-induced map $\pi_1(B^4 \setminus D) \cong \pi_1(B^4 \setminus \nu D) \rightarrow \pi_1(B^4 \setminus P(D))$ is injective.*

Proof. We begin by recalling a key group-theoretic fact: Given groups H , G , and G' and homomorphisms $f : H \rightarrow G$ and $f' : H \rightarrow G'$, consider the amalgamated product $G *_H G'$. If f and f' are injective, then the natural maps of G and G' into $G *_H G'$ are injective (cf [Rot95, §11]).

For the claim in (a), we may assume that the pattern P is not the identity pattern $S^1 \times \{pt\} \subset S^1 \times D^2$, as that case is trivial. The boundary $\partial \bar{\nu} K$ of the closed tubular neighborhood $\bar{\nu} K$ is an incompressible torus that separates $S^3 \setminus P(K)$ into $S^3 \setminus \nu K$ and $\bar{\nu} K \setminus P(K)$. This gives rise to a decomposition

$$\pi_1(S^3 \setminus P(K)) \cong \pi_1(S^3 \setminus \nu K) *_{\pi_1(\partial \bar{\nu} K)} \pi_1(\bar{\nu} K \setminus P(K)).$$

Since $\bar{\nu} K$ is incompressible, the maps on π_1 induced by including $\partial \bar{\nu} K$ into $S^3 \setminus \nu K$ and $\bar{\nu} K \setminus P(K)$ are injective. It follows that the map $\pi_1(S^3 \setminus K) \cong \pi_1(S^3 \setminus \nu K) \rightarrow \pi_1(S^3 \setminus P(K))$ is also injective.

The argument for (b) is even simpler. Consider the decomposition

$$B^4 \setminus P(D) = (B^4 \setminus \nu D) \cup (\bar{\nu} D \setminus P(D)).$$

As in the proof of Proposition 2.1, the intersection of these two subsets has $\pi_1 \cong \mathbb{Z}$, generated by a meridian μ of D . The inclusion-induced map $\mathbb{Z} \rightarrow \pi_1(B^4 \setminus \nu D)$ is clearly injective, and the fact that P has nonzero winding number implies that the other map $\mathbb{Z} \rightarrow \pi_1(\bar{\nu} D \setminus P(D))$ is also injective. As above, we conclude that the map from $\pi_1(B^4 \setminus D) \cong \pi_1(B^4 \setminus \nu D)$ into the amalgamated product $\pi_1(B^4 \setminus P(D))$ is injective. \square

Recall that the *peripheral map* of a slice disk $D \subset B^4$ is the inclusion-induced map $\pi_1(S^3 \setminus \partial D) \rightarrow \pi_1(B^4 \setminus D)$ (cf [JZ20, Definition 3.9]). Consider the following commutative diagram of peripheral maps.

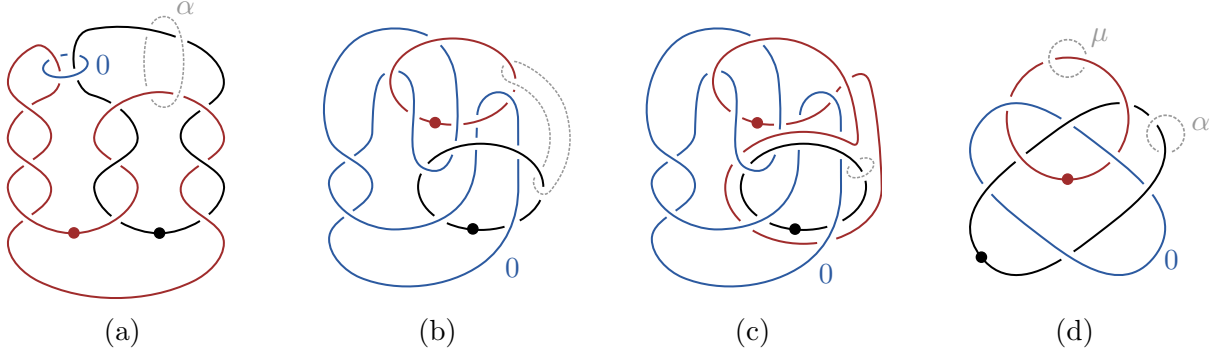


FIGURE 2.2. Handle diagrams for the exterior of the slice disk $D \subset B^4$ bounded by $m(9_{46})$.

$$\begin{array}{ccccc}
 & & \pi_1(B^4 \setminus \nu D) & \longrightarrow & \pi_1(B^4 \setminus P(D)) \\
 & \nearrow & & \nearrow & \\
 \pi_1(S^3 \setminus K) \cong \pi_1(S^3 \setminus \nu K) & \longrightarrow & \pi_1(S^3 \setminus P(K)) & & \\
 & \searrow & & \searrow & \\
 & & \pi_1(B^4 \setminus \nu D') & \longrightarrow & \pi_1(B^4 \setminus P(D'))
 \end{array}$$

When P has nonzero winding number, the horizontal arrows are injective, yielding the following corollary of Proposition 2.3.

Corollary 2.4. *Let $K \subset S^3$ be a knot that bounds slice disks $D, D' \subset B^4$ and let P be a pattern with $P(U) = U$ and $w(P) \neq 0$. If the disks D and D' are distinguished by the kernels of their peripheral maps, then so are the satellite disks $P(D)$ and $P(D')$.*

Example 2.5. Continuing the notation from Example 2.2, we recall the well-known fact that the slice disks D and D' bounded by $m(9_{46})$ are distinguished by their peripheral maps' kernels. To see this, consider Figure 2.2, which exhibits the exterior of $D \subset B^4$. The diagram in part (a) arises from applying the procedure in [GS99, §6.2] to obtain the exterior of $D \subset B^4$, where α is a decorative curve to be used later. Part (b) is obtained by isotopy, and part (c) by sliding one 1-handle over the other. After an isotopy that simplifies the diagram, we obtain (d); in this final diagram, the black and blue curves can be viewed as a handle diagram for B^4 in which D is an unknotted disk bounded by the red curve.

To distinguish the disks D and D' , observe that α is a curve in the knot complement $S^3 \setminus m(9_{46})$ that bounds a smoothly embedded disk in $B^4 \setminus D'$. On the other hand, we claim it is nontrivial in $\pi_1(B^4 \setminus D)$. To see this, choose based representatives of the loops μ and α in Figure 2.2(d). It is straightforward to check that $\pi_1(B^4 \setminus D) \cong \langle \mu, \alpha : \alpha \mu \alpha^{-2} \mu^{-1} \rangle$. This group admits a surjection onto the symmetric group S_3 defined by sending μ to $(2\ 3)$ and α to $(1\ 2\ 3)$ (cf [AKMR15, Proposition 4.4]). It follows that α corresponds to a nontrivial element in $\pi_1(B^4 \setminus D)$, yet it is trivial in $\pi_1(B^4 \setminus D')$ because it bounds a disk in $B^4 \setminus D'$. This implies that the peripheral maps associated to D and D' have distinct kernels, hence these disks are not topologically isotopic rel boundary. By Corollary 2.4, it follows that $P(D)$ and $P(D')$ are not isotopic rel boundary for any unknotted pattern P with nonzero winding number (including, for example, any $(p, 1)$ -cable with $p > 1$).

3. FLOER THEORETIC BACKGROUND

3.1. Knot Floer homology and cobordism maps. Knot Floer homology, defined in [OS04b] and independently in [Ras03], is an invariant of knots, links, and cobordisms between them. In the terminology of [Zem18], link Floer homology associates to a decorated link \mathbf{L} a curved complex $CFL(S^3, \mathbf{L})$ over the commutative ring freely generated over \mathbb{F}_2 by formal variables which correspond to basepoints on the decorated link; to a decorated cobordism it associates a chain map between the curved complexes assigned to its ends. With the aim of being self-contained, we give the definitions of decorated links and cobordisms as well as the category of curved complexes here. For simplicity, we will write “decorated links” rather than *multi-based links with a coloring* as in [Zem18].

Definition 3.1. A *decorated link* is a 5-tuple $\mathbf{L} = (L, \mathbf{w}, \mathbf{z}, P, \sigma)$ which satisfies the following conditions:

- L is a link in S^3
- \mathbf{w} and \mathbf{z} are finite collections of basepoints in L , which intersect nontrivially with every component of L , such that closures of every component of $L \setminus (\mathbf{w} \cup \mathbf{z})$ has one endpoint in \mathbf{w} and the other endpoint in \mathbf{z}
- P is a finite set, and σ is a function from $\mathbf{z} \cup \mathbf{w}$ to P , which defines a “coloring” of the basepoints.

Definition 3.2. For $i = 0, 1$, let $\mathbf{L}_i = (L_i, \mathbf{z}_i, \mathbf{w}_i, P, \sigma_i)$ be decorated links. A *decorated cobordism* between \mathbf{L}_1 and \mathbf{L}_2 is a 5-tuple $\mathbf{S} = (S, \Sigma_z, \Sigma_w, P, \sigma)$ which satisfies the following conditions.

- S is a properly embedded smooth surface in $S^3 \times [0, 1]$, such that $\Sigma \cap (S^3 \times \{i\}) = L_i$ for $i = 0, 1$.
- Σ_w and Σ_z are closed subsurfaces of S such that $\Sigma_w \cup \Sigma_z = S$ and $\Sigma_w \cap \Sigma_z$ is a properly embedded 1-dimensional submanifold of S .
- $L_i \cap \Sigma_w = \mathbf{w}_i$, $L_i \cap \Sigma_z = \mathbf{z}_i$, and $L_i \cap \Sigma_w \cap \mathbf{w}_i$ and $L_i \cap \Sigma_z \cap \mathbf{z}_i$ consist of one point for $i = 0, 1$.
- σ is a function from $\pi_0(\Sigma_w) \cup \pi_0(\Sigma_z)$ to P , such that every basepoint $p \in \mathbf{w}_i \cup \mathbf{z}_i$ which is contained in a connected component $S \in \pi_0(\Sigma_w) \cup \pi_0(\Sigma_z)$ satisfies $\sigma_i(p) = \sigma(S)$ for $i = 0, 1$.

Having defined decorated links and cobordisms, we can describe the algebraic structure of knot Floer homology a bit more precisely. Given a finite set P , consider the commutative ring R_P , freely generated over the field \mathbb{F}_2 by the elements of P . The curved complex $CFL(S^3, \mathbf{L})$ is a bigraded module over R_P . A decorated link cobordism \mathbf{S} between decorated links \mathbf{L}_1 and \mathbf{L}_2 , induces an R_P -linear chain map $F_{\mathbf{S}}$ from $CFL(S^3, \mathbf{L}_1)$ to $CFL(S^3, \mathbf{L}_2)$, which we call the *cobordism map* induced by \mathbf{S} .

In this paper, we will focus on knots, i.e. links with only one component (in which case we denote CFL by CFK instead), and concordances between them, i.e. cobordisms between knots which are homeomorphic to cylinders. We will endow all knots K with the simplest possible decoration, consisting of two basepoints $\mathbf{w} = \{w\}$ and $\mathbf{z} = \{z\}$, two colors $P = \{w, z\}$ and the identity coloring function $\text{id} : \{w\} \cup \{z\} \rightarrow \{w, z\}$. In this case, we have $R_P = \mathbb{F}_2[\mathcal{U}, \mathcal{V}]$ where \mathcal{U} and \mathcal{V} are the formal variables associated to the colors w and z , and the curvature of the complex $CFK(S^3, \mathbf{K})$ vanishes, so that it becomes a chain complex over $\mathbb{F}_2[\mathcal{U}, \mathcal{V}]$.

To make expressions simpler, we will abuse notation, and denote both the knot K and the decorated knot $\mathbf{K} = (K, w, z)$ by K . We will denote by $CFK^\infty(S^3, K)$ the chain complex over $\mathbb{F}_2[\mathcal{U}, \mathcal{U}^{-1}]$ obtained from $CFK(S^3, K)$ by truncating with $\mathcal{V} = 0$ and then localizing by

adjoining the formal inverse of \mathcal{U} . Furthermore, we denote the truncation of $CFK(S^3, K)$ with $\mathcal{U} = \mathcal{V} = 0$ by $\widehat{CFK}(S^3, K)$, and its homology by $\widehat{HFK}(S^3, K)$.

In a similar way, a concordance between knots can be endowed with the simplest possible decoration, so Σ_w and Σ_z are both rectangles. The cobordism map

$$F_S : CFK(S^3, K_1) \rightarrow CFK(S^3, K_2),$$

induced by the decorated cobordism \mathbf{S} , is $\mathbb{F}_2[\mathcal{U}, \mathcal{V}]$ -linear, bidegree-preserving, and induces a quasi-isomorphism on CFK^∞ by [Zem18, Theorem C]. Again, for simplicity, we will simply write S for the decorated concordance described above.

In general, the chain map F_S is not well-defined if a decoration is not specified; due to the ambiguity induced by full rotations along knots, its homotopy class is defined uniquely only up to composition by the basepoint moving map, which was studied by Sarkar in [Sar15], of K_1 (or equivalently, K_2). However, when either K_1 or K_2 is unknotted (which is the context within which we will be working) the map does not depend on the choice of decoration, since the basepoint moving map on the unknot is the identity.

In particular, if S is the concordance obtained by puncturing a slice disk D of a knot K , the chain map

$$F_S : CFK(S^3, U) \rightarrow CFK(S^3, K)$$

is well-defined up to homotopy. Truncating by $\mathcal{U} = \mathcal{V} = 0$ and then taking homology gives a cobordism map

$$\widehat{F}_S : \widehat{HFK}(S^3, U) \rightarrow \widehat{HFK}(S^3, K),$$

which is an invariant of the surface. Since $\widehat{HFK}(S^3, U) \simeq \mathbb{F}_2$, this map can be represented by the homology class

$$t_D := \widehat{F}_S(1) \in \widehat{HFK}(S^3, K).$$

Note that the class t_D depends only on the smooth isotopy class of the given slice disk D . This fact was first observed in [JM16].

3.2. Bordered Floer homology. Bordered Floer homology is a package of invariants of 3-manifolds with boundary [LOT18]. It associates to a surface F a differential graded algebra $\mathcal{A}(F)$ and to a 3-manifold Y parametrized boundary both a type D structure over $\mathcal{A}(-F)$, called $\widehat{CFD}(Y)$, and type A structure over $\mathcal{A}(F)$, called $\widehat{CFA}(Y)$.

Recall that a type D structure over \mathcal{A} is a pair (N, δ^1) where N is a graded \mathbb{F} -module and

$$\delta^1 : N \rightarrow (A \otimes N)[1],$$

is an \mathbb{F} -module map satisfying

$$(\mu_2 \otimes \mathbb{I}_N) \circ (\mathbb{I}_A \otimes \delta^1) \circ \delta^1 + (\mu_1 \otimes \mathbb{I}_N) \circ \delta^1 = 0.$$

We will frequently be interested in *type D structure homomorphisms*, which are \mathbb{F} -module maps $f^1 : N_1 \rightarrow A \otimes N_2$ satisfying

$$(\mu_2 \otimes \mathbb{I}_{N_2}) \circ (\mathbb{I}_A \otimes f^1) \circ \delta_{N_1}^2 + (\mu_2 \otimes \mathbb{I}_{N_2}) \circ (\mathbb{I}_A \otimes \delta_{N_2}^1) \circ f^1 + (\mu_1 \otimes \mathbb{I}_{N_2}) \circ f^1 = 0.$$

The map δ^1 can be iterated to define maps

$$\delta^k : N \rightarrow (A^{\otimes k} \otimes N)[k],$$

where $\delta^0 = \mathbb{I}_N$ and $\delta^k = (\mathbb{I}_{A^{\otimes(k-1)}} \otimes \delta^1) \circ \delta^{k-1}$. Similarly, a type D homomorphism f^1 can be used to define maps

$$f^k : N_1 \rightarrow (A^{\otimes k} \otimes N_2)[k-1], \quad f^k(x) = \sum_{i+j=k-1} (\mathbb{I}_{A^{\otimes(i-1)}} \otimes \delta_{N_2}^j) \circ (\mathbb{I}_{A^{\otimes i}} \otimes f^1) \circ \delta_{N_1}^i.$$

A type A structure is a graded \mathbb{F} -module M equipped with operations

$$m_i : M \otimes A^{\otimes(i-1)} \rightarrow M[2-i],$$

satisfying

$$\begin{aligned} & \sum_{i+j=n+1} m_i(m_j(x \otimes a_1 \otimes \dots \otimes a_{j-1}) \otimes \dots \otimes a_{n-1}) \\ & + \sum_{i+j=n+1} \sum_{\ell=1}^{n-j} \mu_i(x, a_1 \otimes \dots \otimes a_{\ell-1} \otimes \mu_j(a_\ell \otimes \dots \otimes a_{\ell+j-1}) \otimes \dots \otimes a_{n-1}) = 0. \end{aligned}$$

Given both a type A and a type D structure, we define the box tensor product of M and N to be the \mathbb{F} -module $M \boxtimes N = M \otimes_{\mathbb{F}} N$, equipped with differential

$$\partial^{\boxtimes}(x \otimes y) = \sum_{k=0}^{\infty} (m_{k+1} \otimes \mathbb{I}_N)(x \otimes \delta^k(y)).$$

The differential on the box tensor product is often graphically depicted as

$$\partial^{\boxtimes} = \begin{array}{c} \downarrow \qquad \qquad \downarrow \\ \delta \\ \swarrow \\ m \\ \downarrow \qquad \qquad \downarrow \end{array} .$$

Given a map of type D structure $f^1 : N_1 \rightarrow N_2$, we will be interested in maps of the form $\mathbb{I}_M \boxtimes f^1 : M \boxtimes N_1 \rightarrow M \boxtimes N_2$, which are defined as

$$(\mathbb{I}_M \boxtimes f^1)(x \otimes y) = \sum_{k=1}^{\infty} (m_{k+1} \otimes \mathbb{I}_{N_2})(x \otimes f^k(y)).$$

Graphically, these map are given by

$$\mathbb{I}_M \boxtimes f^1 = \begin{array}{c} \downarrow \qquad \qquad \downarrow \\ \delta_{N_1} \\ \swarrow \qquad \qquad \downarrow \\ f^1 \\ \swarrow \qquad \qquad \downarrow \\ \delta_{N_2} \\ \swarrow \\ m \\ \downarrow \qquad \qquad \downarrow \end{array} .$$

The utility of these two algebraic objects is manifest in the bordered Floer homology pairing theorem [LOT18, Theorem 1.3]: if Y_1 and Y_2 are three manifolds with $\partial Y_1 \cong F \cong \partial Y_2$, the

hat-version of the Heegaard Floer homology of $Y_1 \cup_F Y_2$ is recovered by taking the box tensor product of the bordered type A and D structures associated to Y_1 and Y_2 :

$$\widehat{CF}(Y_1 \cup Y_2) \simeq \widehat{CFA}(Y_1) \boxtimes_{\mathcal{A}(F)} \widehat{CFD}(Y_2).$$

Bordered Floer theory also recovers (the $U = 0$ and hat versions of) knot Floer homology [LOT18, Theorem 11.21]: given a doubly pointed bordered Heegaard diagram (\mathcal{H}_1, w, z) for $(Y_1, \partial F, K)$ and a bordered Heegaard diagram (\mathcal{H}_2, z) with $\partial Y_1 \cong F \cong -\partial Y_2$, then

$$\widehat{HFK}(Y_1 \cup Y_2, K) \cong H_*(\widehat{CFA}(\mathcal{H}_1, w, z) \boxtimes_{\mathcal{A}(F)} \widehat{CFD}(\mathcal{H}_2, z)).$$

The analogous version of the pairing theorem for \widehat{HFK}^- will be relevant to us as well. The pairing theorems give an effective way to study satellites: if $P(K)$ is the satellite of K with pattern P , then $\widehat{HFK}(S^3, P(K))$ can be computed by finding a doubly pointed bordered Heegaard diagram \mathcal{H}_P for the pattern P in the solid torus and computing the box tensor product $\widehat{CFA}(\mathcal{H}_P) \boxtimes \widehat{CFD}(S^3 \setminus K)$.

Much in the same way, by passing through bordered Floer homology, we can compute link cobordism maps associated to satellite concordance in terms of the maps associated to the original concordance.

Theorem 3.1 ([Gut22, Theorem 2]). *Let $C : K \rightarrow K'$ be a smooth concordance. Then, there exists a map $F : \widehat{CFD}(S^3 \setminus K) \rightarrow \widehat{CFD}(S^3 \setminus K')$ induced by C , such that for any pattern knot P in the solid torus and a suitable decoration on $P(C)$, the following diagram commutes up to homotopy:*

$$\begin{array}{ccc} \widehat{CFA}(\mathcal{H}_P) \boxtimes \widehat{CFD}(S^3 \setminus K) & \xrightarrow{\simeq} & \widehat{CFK}(S^3, P(K)) \\ \downarrow \mathbb{I}_{\widehat{CFA}(\mathcal{H}_P)} \boxtimes F & & \downarrow F_{P(C)} \\ \widehat{CFA}(\mathcal{H}_P) \boxtimes \widehat{CFD}(S^3 \setminus K') & \xrightarrow{\simeq} & \widehat{CFK}(S^3, P(K')), \end{array}$$

where \mathcal{H}_P is a doubly pointed, bordered Heegaard diagram for $P \subset S^1 \times D^2$, $P(K)$ and $P(K')$ are satellites of K and K' , and $P(C)$ is the satellite concordance induced by P . The horizontal arrows are given by the pairing theorem [LOT18]. The analogous statement for \widehat{CFK}^- holds as well.

4. DISK MAPS AND SATELLITE OPERATORS

In this section, we prove the key proposition which will lead to the proof of Theorem A.

Proposition 4.1. *Let K be a knot in S^3 and let D_1 and D_2 be a pair of slice disks for K . If the invariants t_{D_1} and t_{D_2} are distinct in $\widehat{HFK}(S^3, K)$, then for any knot J and $s < 2\tau(J)$, $t_{P_{J,s}(D_1)}$ and $t_{P_{J,s}(D_2)}$ are distinct as well.*

We begin by giving a simple criterion for determining when an unknotted pattern P is guaranteed to produce \widehat{HFK} -distinguishable disks in terms of the structure of $\widehat{CFA}(S^1 \times D^2, P)$.

When P is an unknotted pattern, we have that

$$\widehat{CFA}(S^1 \times D^2, P) \boxtimes \widehat{CFD}(S^3 \setminus U) \simeq \widehat{CFK}(S^3, U).$$

Therefore, there is some element a in $\widehat{CFA}(S^1 \times D^2, P)$ such that $a \otimes v$ generates homology of $\widehat{CFK}(S^3, U)$, where v is the unique element in $\widehat{CFD}(S^3 \setminus U)$. On homology, $\mathbb{I}_P \boxtimes F$ is therefore determined by the image of $a \otimes v$.

Lemma 4.2 (No cancellation lemma). *Let*

$$F : \widehat{CFD}(S^3 \setminus U) \rightarrow \widehat{CFD}(S^3 \setminus K),$$

be a morphism of type D structures which tensors with the identity map of $\widehat{CFA}(S^1 \times D^2, \lambda)$ to give a nontrivial map, where λ is the knot $S^1 \times \{pt\} \subset S^1 \times D^2$. Let a be an element of $\widehat{CFA}(S^1 \times D^2, P)$ such that $a \otimes v$ generates the homology of $\widehat{CFA}(S^1 \times D^2, P) \boxtimes \widehat{CFD}(S^3 \setminus U)$ and extend $\{a\}$ to a basis for $\widehat{CFA}(S^1 \times D^2, P)$. If the coefficient of a is zero in every \mathcal{A}_∞ operation $m_k(b, \rho_{i_1}, \dots, \rho_{i_{k-1}})$ of $\widehat{CFA}(S^1 \times D^2, P)$ which preserves the filtration, then the map

$$\mathbb{I}_P \boxtimes F : H_*(\widehat{CFA}(S^1 \times D^2, P) \boxtimes \widehat{CFD}(S^3 \setminus U)) \rightarrow H_*(\widehat{CFA}(S^1 \times D^2, P) \boxtimes \widehat{CFD}(S^3 \setminus K))$$

is nontrivial.

Proof. Let $x = F(v)$, where F is the map of type D structures induced by F_C . We can write

$$x = 1 \cdot \theta + \sum_{I \in \{1,2,3,12,23,123\}} \rho_I \theta_I,$$

for some $\theta_I \in \widehat{CFD}(S^3 \setminus K)$. The term θ must be nontrivial, since we have assumed that $\mathbb{I}_{\widehat{CFA}(S^1 \times D^2, \lambda)} \boxtimes F$ has nontrivial image (this follows from the fact that $\widehat{CFA}(S^1 \times D^2, \lambda)$ has no nontrivial \mathcal{A}_∞ -operations and so all other terms in $F(x)$ are annihilated after taking the box tensor product.) $(\mathbb{I}_P \boxtimes F)(a \otimes v)$ is defined to be

$$\begin{aligned} (\mathbb{I}_P \boxtimes F)(a \otimes v) &= \sum_{k=1}^{\infty} (m_{k+1} \otimes \mathbb{I}_P) \circ (a \otimes F^k(v)) \\ &= a \otimes \theta + \text{other terms.} \end{aligned}$$

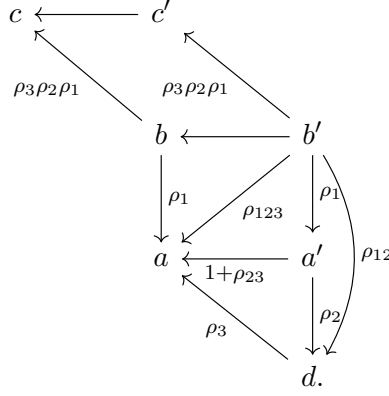
The term $a \otimes \theta$ could be canceled if, for some k , $F^k(v) = \rho_{i_1} \otimes \dots \otimes \rho_{i_k} \otimes \theta$ and there is an operation of the form $m_{k+1}(a, \rho_{i_1}, \dots, \rho_{i_k})$ in which a appears with nonzero coefficient. However, we have assumed that no such operations exist.

Moreover, when we pass to homology, there are no relations between $a \otimes \theta$ and any other elements of $H_*(\widehat{CFA}(S^1 \times D^2, P) \boxtimes \widehat{CFD}(S^3 \setminus K))$, since $a \otimes \theta$ could only appear as a term in the boundary of another element if there were a filtration preserving operation of the form $m_{k+1}(b, \rho_{i_1}, \dots, \rho_{i_k})$ in which a appeared with nonzero coefficient. Again, no such operations exist.

Therefore, $a \otimes \theta$ appears as a non-canceling term in the expansion of $(\mathbb{I}_P \boxtimes F)(a \otimes v) \in H_*(\widehat{CFA}(S^1 \times D^2, P) \boxtimes \widehat{CFD}(S^3 \setminus K))$, from which it follows that $\mathbb{I}_P \boxtimes F$ has nontrivial image. \square

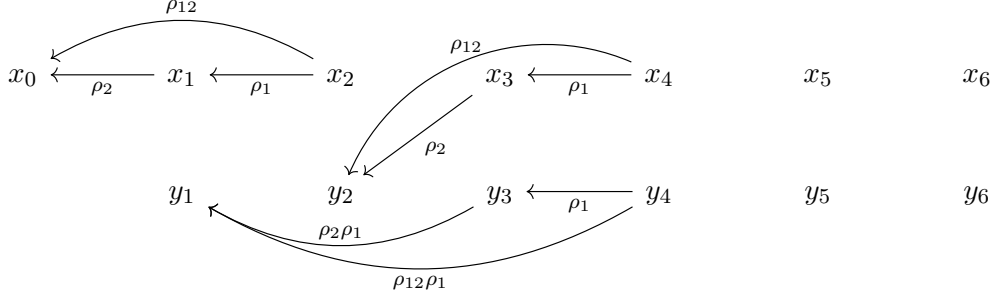
Therefore, to show knot Floer homology will continue to distinguish slice disks after applying an unknotted pattern P , it suffices to show the type A structure of the pattern satisfies the hypotheses of Lemma 4.2. To demonstrate this process, we consider several concrete examples.

Example 4.3. The type A structure for the positive Whitehead double is computed by Levine [Lev12] and is shown below:



In the diagram above, an arrow of the form $x \xrightarrow{\rho_{i_1} \dots \rho_{i_k}} y$ indicates that $m_{k+1}(x, \rho_{i_1}, \dots, \rho_{i_k}) = y$. Arrows pointing left lower the filtration. A short computation shows that $H_*(\widehat{CFA}(S^1 \times D^2, \text{Wh}) \boxtimes \widehat{CFD}(S^3 \setminus U)) = \mathbb{F}\langle b \otimes v \rangle$. By Lemma 4.2, we can verify the nontriviality of $\mathbb{I}_{\text{Wh}} \boxtimes (F_1 + F_2)$ by simply analyzing those \mathcal{A}_∞ operations which output b , i.e. those arrows which point into b . Clearly, there is one such arrow, as b appears in $m_1(b')$, but this operation lowers the filtration level. Therefore, by Lemma 4.2, the map $\mathbb{I}_{\text{Wh}} \boxtimes (F_1 + F_2)$ must be nontrivial.

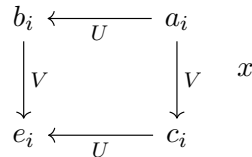
Example 4.4. As another example, consider the Mazur pattern M . The type A structure for the Mazur pattern was computed in [PW21], and the $U = 0$ truncation is shown below.



Here, $\iota_0 \cdot \widehat{CFA}(S^1 \times D^2, M) = \langle x_0, x_2, x_4, y_0, y_2, y_4 \rangle$ and the homology of $\widehat{CFA}(S^1 \times D^2, M) \boxtimes \widehat{CFD}(S^3 \setminus U)$ is generated by $y_4 \otimes v$. In this example, there are no arrows into y_4 at all. Therefore, \widehat{HFK} -distinguishable disks will remain distinguishable after applying the Mazur pattern.

Of course, not all unknotted satellite patterns satisfy the hypotheses of the “no cancellation lemma”, and this failure can give rise to disks which are distinguishable by knot Floer homology, but have satellites which are not.

Example 4.5. Consider our running example, $K = m(9_{46})$. The knot Floer homology calculator [Sza] computes that $CFK(K)$ consists of a singleton x and two unit boxes, generated by elements a_i, b_i, c_i, e_i for $i \in \{1, 2\}$.



The elements x, e_i are in bigrading $(0, 0)$. Since the two slice disks, D and D' , for K are symmetric, the work of Dai-Hedden-Mallick [DHM21] can be applied to show that

$$t_D + t_{D'} = e_1 + e_2 \in \widehat{CFK}(K).$$

Hence, the two symmetric slice disks for $m(9_{46})$ can be distinguished by knot Floer homology. See [Gut22, Proposition 4.1] for a more detailed computation.

This basis for $CFK(K)$ induces a basis for $\widehat{CFD}(S^3 \setminus K)$ by [LOT18, Theorem 11.26], which is shown below:

$$\begin{array}{ccccc}
 b_i & \xleftarrow{\rho_2} & y_i^1 & \xleftarrow{\rho_3} & a_i \\
 \downarrow \rho_1 & & & & \downarrow \rho_1 \\
 y_i^2 & & & & y_i^4 \\
 \uparrow \rho_{123} & & & & \uparrow \rho_{123} \\
 e_i & \xleftarrow{\rho_2} & y_i^3 & \xleftarrow{\rho_3} & c_i
 \end{array}
 \quad x \curvearrowright \rho_{12}$$

By Theorem 3.1, there is an induced map of type D structures (in fact, there is a unique map in this case), and it is given by

$$F : \widehat{CFD}(S^3 \setminus U) \rightarrow \widehat{CFD}(S^3 \setminus K), \quad v \mapsto e + \rho_3 y^2 + \rho_1 y^3,$$

where $w = w_1 + w_2$, for $w \in \{e, y^2, y^3\}$.

Consider the $(2, -1)$ cabling pattern, which we denote $C_{2,-1}$. The type A structure is computed in [OSS17, Section 8] and is shown below:

$$\begin{array}{ccc}
 & \xrightarrow{\rho_2 \rho_{12}} & A_2 \xleftarrow{\rho_2 \rho_1} A_1 \\
 & \searrow \rho_2 & \downarrow \rho_{23} \\
 X & & B_2 \\
 & \searrow \rho_3 & \nearrow \rho_2 \rho_{123} \\
 & & B_1
 \end{array}$$

The element X is the sole basis element in $\iota_0 \cdot \widehat{CFA}(S^1 \times D^2, C_{2,-1})$. Therefore, we see that

$$(\mathbb{I}_{\widehat{CFA}(S^1 \times D^2, C_{2,-1})} \boxtimes F)(X \otimes v) = X \otimes e + B_2 \otimes y^2.$$

However, this element vanishes on homology. Note that

$$\partial^{\boxtimes}(A^2 \otimes y^3) = (m_2 \otimes \mathbb{I}_{\widehat{CFD}(S^3 \setminus K)})(A^2 \otimes \delta^1(y^3)) = m_2(A^2 \otimes \rho_2) \otimes e = X \otimes e$$

and

$$\partial^{\boxtimes}(A^1 \otimes y^3) = (m_3 \otimes \mathbb{I}_{\widehat{CFD}(S^3 \setminus K)})(A^1, \delta^2(y^3)) = m_3(A^1, \rho_2, \rho_{123}) \otimes y^2 = B_2 \otimes y^2.$$

In fact, by considering the type A structure for $C_{p,-1}$ (see [OSS17, Section 8]), we see that the same argument holds for any positive p . This example is in strong contrast to the behavior of positive cabling patterns; see Section 4.2.

Let us now turn to Levine's infinite family of doubling patterns.

Proof of Proposition 4.1. The type A structure associated to the pattern $P_{J,s}$ in the solid torus, which we denote $\widehat{CFA}(S^1 \times D^2, P_{J,s})$, is computed by Levine. As the knot J is unspecified, the computation is quite complicated. We will only need to consider a small subset of the \mathcal{A}_∞ -operations, so we will only provide a terse description of this module, and refer the careful reader to [Lev12, Section 3].

When $s < 2\tau(J)$, the type A structure $\widehat{CFA}(S^1 \times D^2, P_{J,s})$ is generated by elements

$$A^j, A'^j, B^j, B'^j, C^j, C'^j, D^j, D'^j, E_i^j, E_i'^j, F_i^j, F_i'^j, G_i^j, G_i'^j, H_i^j, H_i'^j,$$

where $0 \leq j \leq \text{rank}(\iota_0 \cdot \widehat{CFD}(S^3 \setminus J))$ and $1 \leq i \leq k_j$, where k_j is the length of the arrow between the $(2j-1)^{\text{th}}$ and $(2j)^{\text{th}}$ generators of $\iota_0 \cdot \widehat{CFD}(S^3 \setminus J)$.

In this case (where $s < 2\tau(J)$), Levine shows that the homology of $\widehat{CFA}(S^1 \times D^2, P_{J,s}) \boxtimes \widehat{CFD}(S^3 \setminus U)$ is generated by $A^0 \otimes v$, where v is the single generator of $\widehat{CFD}(S^3 \setminus U)$. Since we are only interested in the image of this element under the maps induced by the doubles of the disks in consideration, it suffices to consider those \mathcal{A}_∞ -operations with outputs of the form

$$A^0 + \text{other terms.}$$

There is only one such operation,

$$m_1(A^0) = A^0,$$

but this operation does not preserve the filtration (see [Lev12, Figure 22]). Basis elements are arranged in columns according to the Alexander filtration). Therefore, all criteria of Lemma 4.2 are satisfied, so Proposition 4.1 follows. \square

4.1. Disks distinguished by knot Floer homology. From Theorem A, we see that to construct exotic disks bounding $P_{J,s}(K)$, it suffices to construct two slice disks of K which are distinguished by their induced maps on knot Floer homology. It is very easy to find such examples; a systematic way of finding them comes from a 4-dimensional construction called *deformation-spinning*, which we now recall.

Definition 4.6. Let a be a properly embedded smooth arc in D^3 . Furthermore, let $\phi: I \times D^3 \rightarrow D^3$ be an isotopy of D^3 such that $\phi_0 = \text{id}_{D^3}$, $\phi_t|_{\partial D^3} = \text{id}_{\partial D^3}$ for every $t \in I$, and $\phi_1(a) = a$. Then the *deform-spun* slice disk $D_{a,\phi} \subset D^4$ is defined by taking

$$\bigcup_{t \in I} \{t\} \times \phi_t(a) \subset I \times D^3,$$

and rounding the corners along $\{0, 1\} \times \partial D^3$. When the arc a is understood, we simply write D_ϕ instead of $D_{a,\phi}$.

It was observed in [JZ20, Lemma 3.3] that given an (orientation-preserving) self-diffeomorphism d of (D^3, a) such that $d|_{\partial D^3} = \text{id}_{\partial D^3}$, there exists an isotopy $\phi: I \times D^3 \rightarrow D^3$, such that $\phi_1 = d$. Furthermore, the isotopy class of the deform-spun disk $D_{a,\phi}$ only depends on d . Hence we will denote $D_{a,\phi}$ by $D_{a,d}$ for simplicity. Moreover, by [JZ20, Theorem 5.1], the element $t_{D_{a,d}}$ is determined by the action of d_* on the knot Floer complex.

Definition 4.7. Let K be a knot in S^3 , and suppose that the open 3-ball B intersects K in an unknotted arc. Then $(S^3 \setminus B, K \setminus B)$ is diffeomorphic to a ball-arc pair (D^3, a) . Suppose that we are given a diffeomorphism $d \in \text{Diff}(S^3, K)$ that is the identity on B . Then the *deform-spun* slice disk $D_{K,d} \subset B^4$ for $-K \# K$ is defined to be $D_{a,d|_{S^3 \setminus B}}$.

Now we are able to prove Corollary A.2.

Proof of Corollary A.2. Consider the diffeomorphism $R^\pi : (S^3, K \# K) \rightarrow (S^3, K \# K)$ which swaps the two summands of $K \# K$ as in Figure 4.1. The action of R^π on $\widehat{HFK}(S^3, K \# K)$ (or more generally, $HFK^\infty(S^3, K)$) was identified in [JZ21, Theorem 8.1] as

$$(R^\pi)_* = \text{Sw} \circ (1 \otimes (1 + \Psi\Phi) + \Psi \otimes \Phi),$$

where Sw denotes the automorphism of the group

$$\widehat{HFK}(S^3, K \# K) \simeq \widehat{HFK}(S^3, K) \otimes \widehat{HF}(S^3, K)$$

which switches the two $\widehat{HFK}(S^3, K)$ factors.

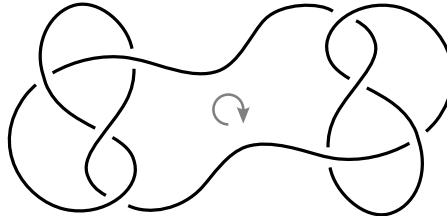


FIGURE 4.1. The knot $K \# K$, when K is the figure-eight knot in this figure. The diffeomorphism R^π acts by 180° rotation in the plane.

Choose any nonzero element $a_0 \in \widehat{HFK}(S^3, K)$. If $\Phi(a_0) = 0$, then we define $a = a_0$; otherwise we take $a = \Phi(a_0)$, so that $\Phi(a) = \Phi^2(a_0) = 0$ since $\Phi^2 = 0$ [Zem18, Lemma 4.9]. Since the hat version of knot Floer homology detects the unknot [OS04a], we can find a nonzero element $b \in \widehat{HFK}(S^3, K)$ which is different from a . Then we have

$$(R^\pi)_*(b \otimes a) = \text{Sw}(b \otimes a) = a \otimes b.$$

Since $a \neq b$ and a, b are both nonzero, we see that $(R^\pi)_*$ is not homotopic to the identity. From [JZ20, Theorem 5.1], we then see that the deform-spun slice disks $D_{K \# K, R^\pi}$ and $D_{K \# K, \text{id}}$ of $K \# K \# -K \# -K$, induced by the diffeomorphisms R^π and id , satisfy $t_{D_{K \# K, R^\pi}} \neq t_{D_{K \# K, \text{id}}}$ in $\widehat{HFK}(S^3, K \# K \# -K \# -K)$. Therefore, by Theorem A, the slice disks $P_{J,s}(D_{K \# K, R^\pi})$ and $P_{J,s}(D_{K \# K, \text{id}})$ are topologically isotopic but not smoothly isotopic. \square

4.2. Cables and Stabilization Distance. We will now use the same strategy to prove Theorem B. The type A structure for the $(p, 1)$ cabling pattern, $C_{p,1}$, was computed in [Hom14] (here, we consider the case $p \geq 1$). $CFA^-(S^1 \times D^2, C_{p,1})$ is generated by a, b_1, \dots, b_{2p-2} , and

the A_∞ operations are given as follows:

$$\begin{aligned}
m_{3+i}(a, \rho_3, \overbrace{\rho_{23}, \dots, \rho_{23}}^i, \rho_2) &= U^{pi+p}a, \quad i \geq 0, \\
m_{4+i+j}(a, \rho_3, \overbrace{\rho_{23}, \dots, \rho_{23}}^i, \rho_2, \overbrace{\rho_{12}, \dots, \rho_{12}}^j, \rho_1) &= U^{pi+j+1}b_{j+1}, \quad 0 \leq j \leq p-2, i \geq 0, \\
m_{2+j}(a, \overbrace{\rho_{12}, \dots, \rho_{12}}^j, \rho_1) &= b_{2p-j-2}, \quad 0 \leq j \leq p-2, \\
m_1(b_j) &= U^{p-j}b_{2p-j-1}, \quad 1 \leq j \leq p-1, \\
m_{3+i}(b_j, \rho_2, \overbrace{\rho_{12}, \dots, \rho_{12}}^i, \rho_1) &= U^{i+1}b_{j+i+1}, \quad 1 \leq j \leq p-2, 0 \leq i \leq p-j-2, \\
m_{3+i}(b_j, \rho_2, \overbrace{\rho_{12}, \dots, \rho_{12}}^i, \rho_1) &= b_{j-i-1}, \quad p+1 \leq j \leq 2p-2, 0 \leq i \leq j-p-1.
\end{aligned}$$

Theorem B makes uses of the HFK^- version of the pairing theorem, which states that

$$CFK^-(S^3, K) \simeq CFA^-(S^1 \times D^2, P) \boxtimes \widehat{CFD}(S^3 \setminus K),$$

for a pattern P in the solid torus.

Proof of Theorem B. By Theorem 3.1, we have two type D morphisms

$$f_1, f_2 : \widehat{CFD}(S^3 \setminus U) \rightarrow \widehat{CFD}(S^3 \setminus K)$$

which compute the maps associated to satellites of D_1 and D_2 . Let $x = f_1(v) + f_2(v)$, where v is the single generator of $\widehat{CFD}(S^3 \setminus U)$, and write

$$x = \theta + \sum_{J \in \{1,2,3,12,23,123\}} \rho_J \theta_J,$$

as in the proof of Lemma 4.2. Since $t_{D_1} + t_{D_2} \neq 0$ in $\widehat{HFK}(S^3, K)$, we know that θ is nonzero. Since the homology of the chain complex

$$\mathbb{F}_2[U] \simeq CFK^-(S^3, U) \simeq CFA^-(S^1 \times D^2, C_{p,1}) \boxtimes \widehat{CFD}(S^3 \setminus U)$$

is generated by $a \otimes v$, we know that $t_{(D_1)_{p,1}} + t_{(D_2)_{p,1}}$ is the homology class of

$$(\text{id}_{CFA^-(S^1 \times D^2, C_{p,1})} \boxtimes (f_1 + f_2))(a \otimes v),$$

which contains the term $a \otimes \theta$. Since any A_∞ operation in $CFA^-(S^1 \times D^2, C_{p,1})$ which has some $\mathbb{F}_2[U]$ -multiple of a as an output has coefficients of the form U^{pi+p} for some $i \geq 0$, it is clear from the no-cancellation argument of Lemma 4.2 that $U^k(t_{(D_1)_{p,1}} + t_{(D_2)_{p,1}})$ is nonvanishing in homology whenever $0 \leq k < p$. It then follows from [JZ21, Theorem 1.1] that the stabilization distance between $(D_1)_{p,1}$ and $(D_2)_{p,1}$ is at least p . \square

5. AN INFINITE FAMILY OF EXOTIC SLICE DISKS

As discussed in §1.2, the techniques developed above are insufficient to distinguish infinite families of pairwise exotic slice disks. Nevertheless, those methods suggest that $\text{Wh}(4_1 \# 4_1)$ should bound infinitely many exotic slice disks. Instead, we are able to detect this family via an indirect application of Seiberg-Witten invariants.

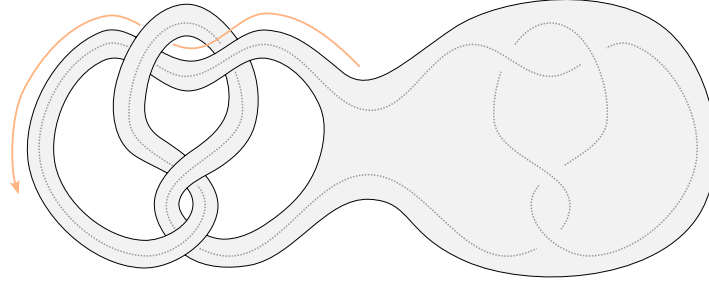


FIGURE 5.1. An incompressible swallow-follow torus in the complement of $K = 4_1\# - 4_1$, decorated with an arrow to indicate the swallow-follow isotopy.

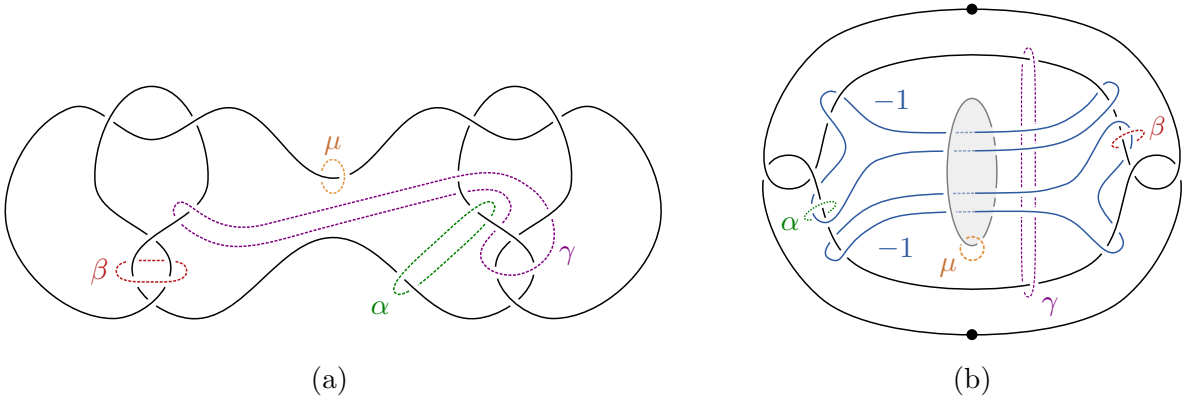


FIGURE 5.2. (a) Decorated curves in the complement of $K = 4_1\# - 4_1$. (b) A nonstandard handle diagram for B^4 in which K is unknotted and its slice disk (shown in gray) is standard.

Proof of Theorem C. Let K denote the knot $4_1\# - 4_1$, and let D denote its standard slice disk. Consider the isotopy from K to itself given by a longitudinal twist along one of the swallow-follow tori in $S^3 \setminus K$ as depicted in Figure 5.1. Dragging D along by any extension of this isotopy to B^4 and repeating n times, we obtain a family of ribbon disks D_n for K . These disks D_n themselves are not exotic, and they can be distinguished using elementary techniques (e.g., by their inclusion-induced peripheral maps $\pi_1(S^3 \setminus K) \rightarrow \pi_1(B^4 \setminus D_n)$, cf [Fox66, JZ20]). However, by passing indirectly through a construction due to Gompf [Gom17a], they can also be distinguished using Seiberg-Witten invariants. We will show that this latter perspective enables us to distinguish the doubled disks $\text{Wh}(D_n)$, which are topologically isotopic rel boundary by [CP21a].

In [Gom17a] (cf [Gom17b, Akb17]), Gompf shows that the contractible 4-manifold W obtained from the exterior of $D \subset B^4$ by attaching a (-1) -framed 2-handle along a meridian of K is an infinite-order cork, where the twisting automorphism of ∂W is induced by the aforementioned torus twist in $S^3 \setminus K$. This can be reframed using the disks D_n : Given an embedding of W into a larger 4-manifold Z , cutting out $W \subset Z$ and regluing by the torus twist is equivalent to simply replacing $W \subset X$ with the 4-manifold W_n given by attaching a (-1) -framed meridional 2-handle to the exterior of D_n in B^4 .

We recall the relevant parts of Gompf's argument, borrowing aspects of Akbulut's exposition in [Akb17]. Part (a) of Figure 5.2 shows K decorated with four curves α , β , γ , and μ , the last

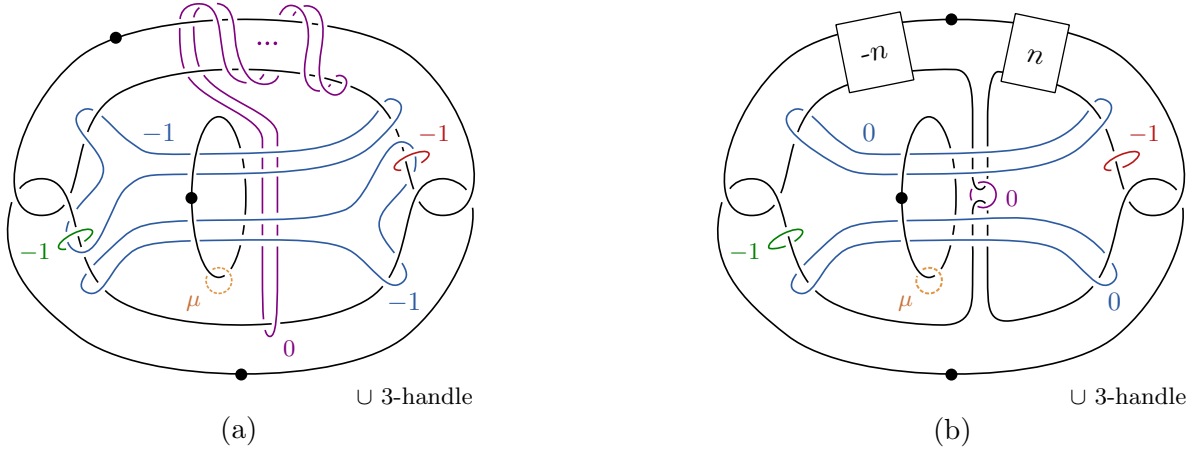


FIGURE 5.3. Diagrams for the 4-manifold X_n obtained by attaching additional handles to the exterior of the disk $D_n \subset B^4$.

of which is a meridian of K . Part (b) of Figure 5.2 recasts the situation using a nonstandard handle diagram of B^4 in which K and D are unknotted. With framings specified relative to this nonstandard diagram, attach 2-handles to $B^4 \setminus \nu D$ along α and β with framing -1 and along γ with framing 0 . (Note that, in the standard diagram in part (a), α and β would be 0 -framed and γ would be (-2) -framed.) It can also be shown that the resulting boundary contains a nonseparating 2-sphere. (This is not obvious from the present diagram but becomes clearer upon using the 2-handles attached along α and β to cancel the 1-handles from our nonstandard handle structure on B^4 . One may then perform simple handleslides to free up a 0 -framed 2-handle attached along an unknot that is split from the rest of the diagram.) We may attach a 3-handle along this nonseparating 2-sphere, yielding a new 4-manifold we denote by X . At present, since we have not pinned down the precise embedding of the nonseparating 2-sphere, we do not claim that X is well-defined. However, this 2-sphere is disjoint from the meridian curve μ , and we will later attach a 2-handle along μ , making the 4-manifold simply connected. The result of attaching the 3-handle will then become well-defined by work of Trace [Tra82].

Let X_n denote the 4-manifold obtained from X by replacing $W \subset X$ with W_n . Equivalently, we can apply the torus twist n times to the attaching curves α , β , and γ before attaching the 2-handles. Observe that γ is the only one of these curves that has essential intersections with the swallow-follow torus, hence we may arrange for the other attaching curves (as well as μ) to be fixed by the torus twist. The resulting 4-manifold X_n can be shown to have the handle diagram shown in Figure 5.3(a) (cf [Gom17b, Figure 11], [Akb17, Figure 5]). After further manipulation (namely straightening out γ and sliding the original 2-handles from B^4 over the 2-handles attached along α and β), we obtain the diagram in Figure 5.3(b). Using the 0 -framed 2-handle attached along γ , we can combine the two dotted curves representing genuine 1-handles in Figure 5.3(b) and replace them with a single knotted curve with a dot. This represents the obvious ribbon complement for the slice knot $\kappa_n \# -\kappa_n$, where κ_n is the n -twist knot. See the left side of Figure 5.4. This is precisely the result of applying the knot surgery operation of Fintushel-Stern [FS98] (using the twist knot κ_n) to the core torus in the simplified picture of X_0 shown on the righthand side of Figure 5.4.

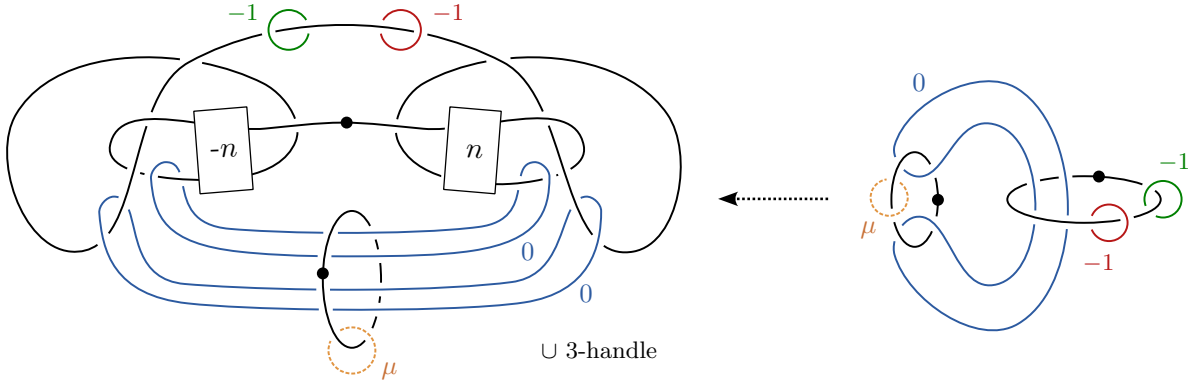
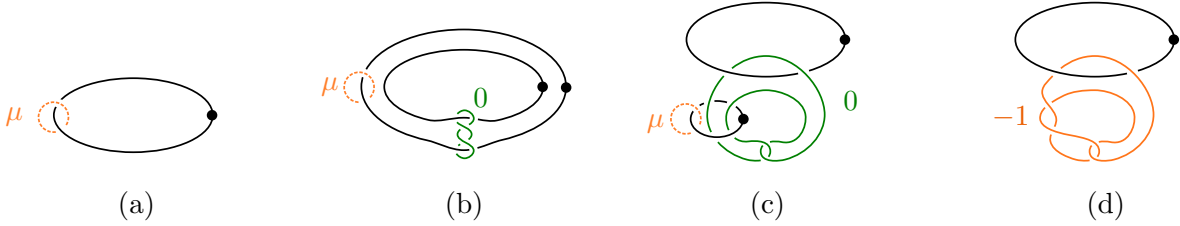
FIGURE 5.4. Realizing X_n as knot surgery on X_0 .

FIGURE 5.5. Part (a) represents the exterior of the unknot's standard slice disk in B^4 ; 2-handles are allowed to pass over the associated 1-handle, but are not pictured. To obtain (b), we replace the exterior of the unknot's standard slice disk with the exterior of its Whitehead double. To obtain (c), we slide the outer 1-handle over the inner 1-handle, then simplify by isotopy. In (d), we illustrate the effect of attaching a (-1) -framed 2-handle along the meridian μ from part (c) and canceling the resulting 1-/2-handle pair.

We may now turn to the matter at hand: Had we applied this process with the Whitehead doubles $\text{Wh}(D_n)$ instead of D_n , we would replace the dotted curve representing D and the meridian curve μ in the manner shown in parts (a)-(c) of Figure 5.5. If we attach a (-1) -framed 2-handle along the new meridian, we may simplify to obtain part (d) of Figure 5.5. We apply this to the 4-manifolds X_n . Moreover, we will also choose to attach a (-1) -framed 2-handle along the old meridian. (This realizes the knot surgery torus as a fiber in a cusp neighborhood.) The result of attaching these additional handles to X_0 is depicted in part (a) of Figure 5.6, and the remaining parts (b) and (c) simplify this handle diagram and show that this 4-manifold admits a Stein handle diagram. It follows that this 4-manifold embeds into a (minimal) closed Kähler surface Z [LM97]. Since the twist knot κ_n has nontrivial Alexander polynomial, the 4-manifolds obtained by performing knot surgery with κ_n along the torus in the cusp fiber all have distinct Seiberg-Witten invariants by [FS98]. (It is clear that the ambient 4-manifold has $b_2^+ > 1$ and that the torus complement is simply connected, hence we may apply [FS98, Theorem 1.5].) It follows that the slice disks $\text{Wh}(D_n)$ are not smoothly isotopic rel boundary. \square

We can upgrade these examples to produce disks that are absolutely exotic, adapting a strategy from [AR16].

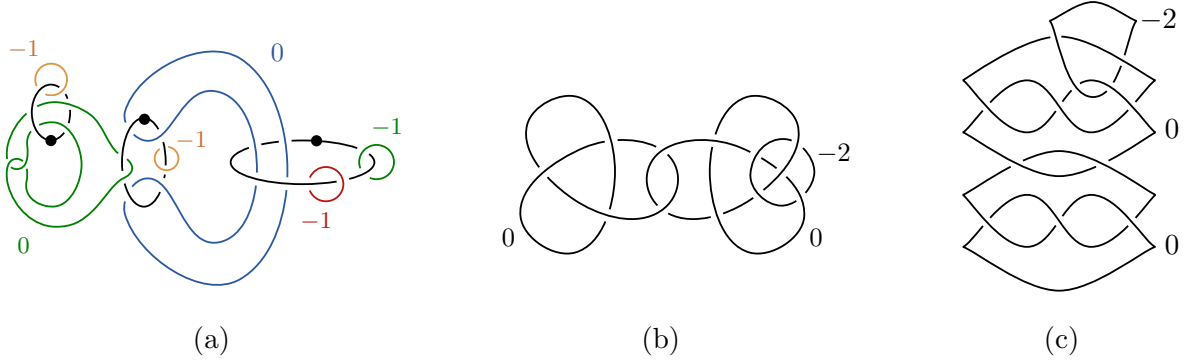


FIGURE 5.6. Diagrams for a 4-manifold obtained by attaching 2-handles to the exterior of $\text{Wh}(D_n) \subset B^4$.

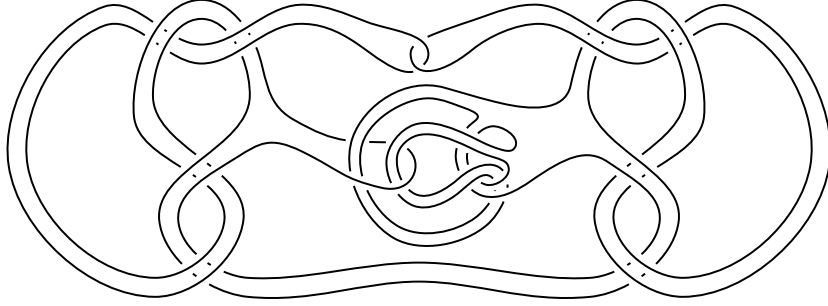


FIGURE 5.7. A knot K' that is concordant to $\text{Wh}(4_1 \# 4_1)$ and bounds an infinite family of absolutely exotic slice disks.

Proof of Corollary C.1. Let K' denote the knot shown in Figure 5.7. A calculation in SnapPy [CDGW] verifies that K' is hyperbolic with trivial isometry group, which further implies that every diffeomorphism of the pair (S^3, K') is isotopic to the identity (through diffeomorphisms of the pair). Note that K' is obtained from $K = \text{Wh}(4_1 \# 4_1)$ by a tangle replacement in the center of the diagram. By [Rub90, Proof of Theorem 2.6], there exists an invertible concordance C from $K = \text{Wh}(4_1 \# 4_1)$ to K' . Here invertibility means that there is a concordance C' from K' to K such that gluing C' to C along K' yields a product, i.e., $C \cup C'$ and $K \times [0, 1]$ are smoothly isotopic rel boundary. Define a family of slice disks $D'_n = \text{Wh}(D_n) \cup C$ bounded by K' . The slice disks $\text{Wh}(D_n)$ are topologically isotopic rel boundary, hence so are the disks D'_n .

Now suppose that D'_n and D'_m are smoothly isotopic, not necessarily rel boundary, for $n \neq m$. Since (S^3, K') has no nontrivial symmetries, we may further assume that D'_n and D'_m are smoothly isotopic rel boundary. It then follows that $D'_n \cup C'$ and $D'_m \cup C'$ are smoothly isotopic rel boundary. But since $C \cup C'$ is isotopic to the product $K \times [0, 1]$ (rel boundary), the disks $D'_n \cup C'$ and $D'_m \cup C'$ can be obtained from $\text{Wh}(D_n)$ and $\text{Wh}(D_m)$ by attaching an extended collar along their boundary. It follows that these extended slice disks are smoothly isotopic rel boundary. However, this implies that the disks $\text{Wh}(D_n)$ and $\text{Wh}(D_m)$ themselves are smoothly isotopic rel boundary, contradicting the results above. We conclude that D'_n and D'_m are not smoothly isotopic whenever $n \neq m$. \square

6. EXOTIC SURFACES WITH DIFFEOMORPHIC BRANCHED COVERS

The goal of this section is to prove Theorem D. We begin with a proposition that helps us understand the branched double covers of certain satellite disks. Here we consider a generalization of Levine's patterns $P_{J,k}$ to the case where k is a half-integer. To state it, we recall the definition of $1/k$ -surgery on a slice disk: Given a smooth slice disk $D \subset B^4$, fix a compact tubular neighborhood $\bar{\nu}D \cong D \times D^2$ and a choice of meridian μ of $\partial D \subset S^3$. By taking the disk exterior $B^4 \setminus \nu D$ and attaching a $(-k)$ -framed 2-handle along μ , we obtain a contractible 4-manifold bounded by $S^3_{1/k}(\partial D)$. We refer to this 4-manifold as $1/k$ -surgery along the slice disk $D \subset B^4$ and denote it by $B^4_{1/k}(D)$.

- Proposition 6.1.** (a) *For any slice disk D in B^4 , the branched double cover $\Sigma_2(B^4, D_{2,1})$ of the $(2,1)$ -cable $D_{2,1}$ of D is diffeomorphic to $B^4_{+1}(D \natural D^r)$.*
 (b) *More generally, let $D \subset B^4$ be a slice disk and $\mu \in S^3 \setminus \partial D$ a meridian of its boundary. For any knot J , half-integer $k \in \frac{1}{2}\mathbb{Z}$, and associated doubling pattern $P_{J,k}$, the branched double cover $\Sigma_2(B^4, P_{J,k}(D))$ is diffeomorphic to $(B^4 \setminus \nu(D \natural D^r)) \cup h$, where h is a $2k$ -framed 2-handle attached along $\mu \# J \# J^r$ and $\nu(\cdot)$ denotes an open tubular neighborhood.*

Proof. The first claim in the proposition is a special case of the latter claim where J is an unknot and $k = -1/2$, so we focus on the more general claim. The proof is essentially given in Figure 6.1, which we unpack below.

Begin by fixing a handle decomposition of B^4 in which the original disk D is represented by a standard slice disk bounded by the unknot. This is depicted schematically in part (a) of Figure 6.1. The gray arcs represent the other handles that are present in the handle decomposition. In part (b) of Figure 6.1, we use this same handle diagram to illustrate the satellite disk $P_{J,k}(D)$. In part (c), we modify the handle diagram to represent the exterior of $P_{J,k}(D)$ in B^4 (see [GS99, §6.2]). The diagram in (d) is obtained by isotopy, (e) is obtained by sliding one 1-handle over the other, and (f) is obtained by further isotopy. In part (g), we depict the branched double cover (see [AK80] or [GS99, §6.3]). (We note that we have assumed $2k$ is even in the figure. If $2k$ is odd, then the colors on the bottoms of the red and blue 2-handles are reversed.) The main detail to verify in this step is the framing data for the 2-handles in part (g), which we now explain.

First consider the framed attaching curve in the center of the diagram in part (f), which we denote by γ . To pin down what occurs in the (J, k) -tangle, fix a diagram of J as a knotted arc with c crossings and writhe w . We may construct the (J, k) -tangle so that its two strands contribute a total of $4c + 2|w| + 2|k|$ crossings, where $4c$ crossings come from adding a blackboard-framed pushoff to the underlying diagram of J , the next $2|w|$ crossings correct for the difference between the blackboard framing and 0-framing, and the final $2|k|$ crossings add the desired twisting in the (J, k) -tangle. We claim the writhe of γ is $2w - 2k$: The strands in the tangle have antiparallel orientation, so the first $4c$ crossings cancel in sign; if the strands had parallel orientation, the next $2|w|$ crossings would contribute a signed total of $-2w$ crossings, but instead contribute $2w$ because of the antiparallel orientation; similarly, if the strands had parallel orientations, the final $2|k|$ crossings would contribute $2k$ to the writhe, but instead contribute $-2k$. Thus the writhe of γ is $2w - 2k$, hence the 0-framing curve differs from the blackboard framing by $-(2w - 2k) = 2k - 2w$ full signed twists.

Now we consider the lift $\tilde{\gamma}$ of γ in the branched double cover, which consists of two framed components. Each component of $\tilde{\gamma}$ has $2c$ self-crossings (from passing through both (J, k) -tangles), with writhe given by $2w$. The framing from γ lifts to a framing on each component

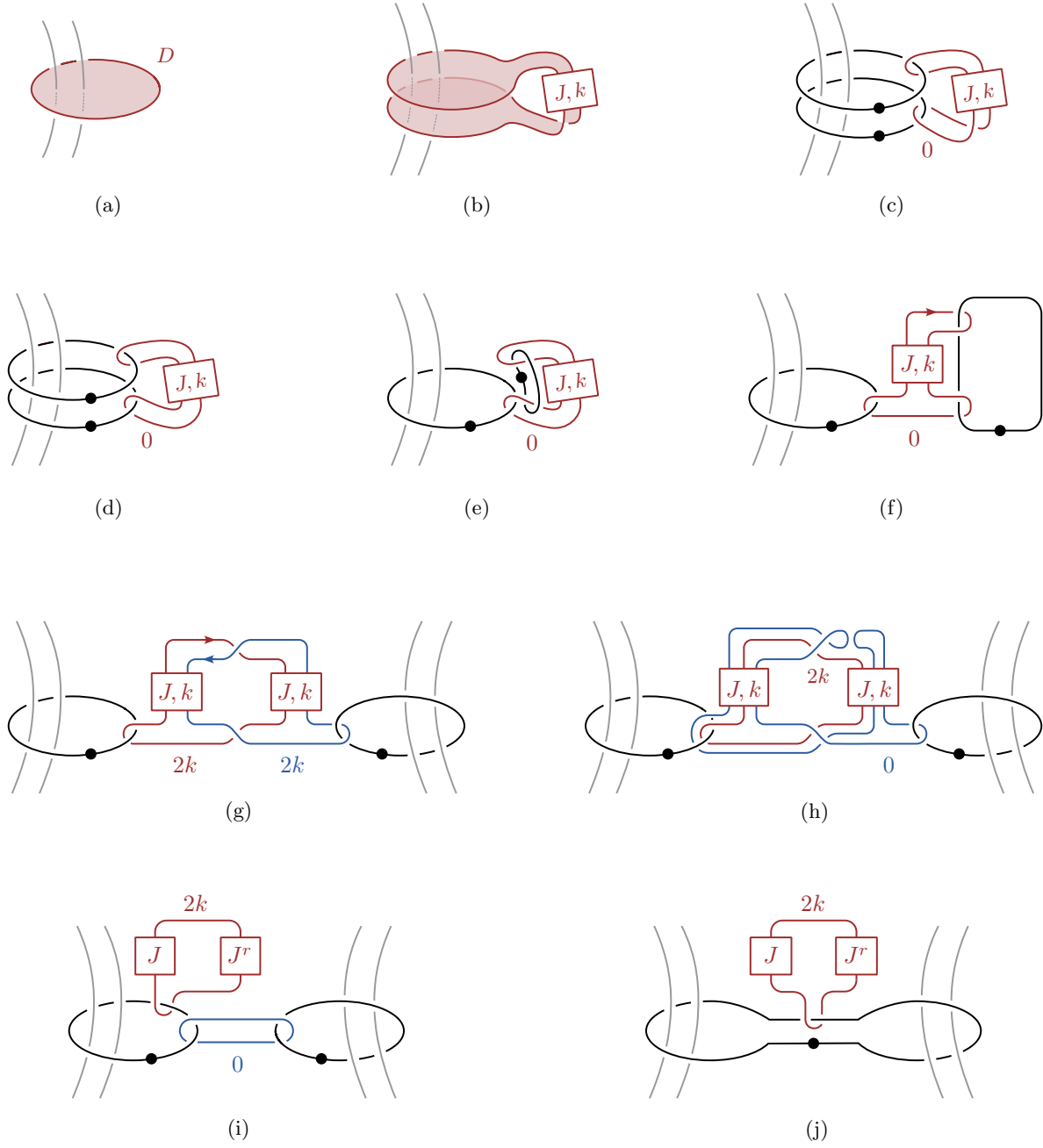


FIGURE 6.1. (a) The disk D depicted schematically in a nonstandard handle diagram of B^4 . (b) The satellite disk $P_{J,k}(D)$. (c)-(f) Handle diagrams for the exterior of $P_{J,k}(D)$ in B^4 . (g)-(j) Handle diagrams for the branched double cover $\Sigma_2(B^4, P_{J,k}(D))$.

of $\tilde{\gamma}$, hence each lifted framing differ from the blackboard framing by adding $2k - 2w$ signed full twists. Since the blackboard framing on each component is $2w$, it follows that the lifted framing on each component of $\tilde{\gamma}$ is $2k$, as claimed in the diagram in part (g).

Next, we slide one of the components of $\tilde{\gamma}$ over the other component to obtain the diagram in (h), then perform an isotopy that pulls the modified components out of the (J, k) -tangle boxes to obtain the diagram in (i). (To check these steps, it is easiest to work backwards from (i) to (g) by sliding the 0-framed component over the $2k$ -framed component so that the former becomes unlinked from the 1-handle on the left.) Finally, we slide one of the 1-handles in (i) over the other so that the 0-framed component becomes a 0-framed meridian to whichever dotted circle represents the unmodified 1-handle. We may then slide all other 2-handles off of the latter 1-handle curve until it can be canceled with its 0-framed meridian curve, yielding the diagram in part (j). This final diagram is easily recognized as the result of attaching a $2k$ -framed 2-handle to the exterior of $D \natural D' \subset B^4$ along $\mu \# J \# J^r$, where μ is a meridian of the disk's boundary. \square

We point out that branched covers of satellite disks give rise to many examples of exotic contractible 4-manifolds. This can be true even when the satellite disks themselves are not exotically knotted, as the next example illustrates.

Example 6.2. In Example 2.5, it was observed that the standard slice disks D and D' bounded by the knot $K = m(9_{46})$ remain topologically distinct after applying any satellite pattern with nonzero winding number. Nevertheless, for many of the knot doubling patterns $P_{J,k}$, these topologically distinct disks $P_{J,k}(D)$ and $P_{J,k}(D')$ have exotic branched double covers.

To see this, fix a knot J and a half-integer $k \in \frac{1}{2}\mathbb{Z}$ such that $J \# J^r$ has maximal Thurston-Bennequin number $\overline{tb}(J \# J^r) > 2k$. Following Proposition 6.1, we produce a handle diagram for the branched double cover $W = \Sigma_2(B^4, P_{J,k}(D))$ in Figure 6.2(a-c), where $T = J \# J^r$. In particular, the initial diagram in part (a) was obtained earlier in Figure 2.2, which depicts D

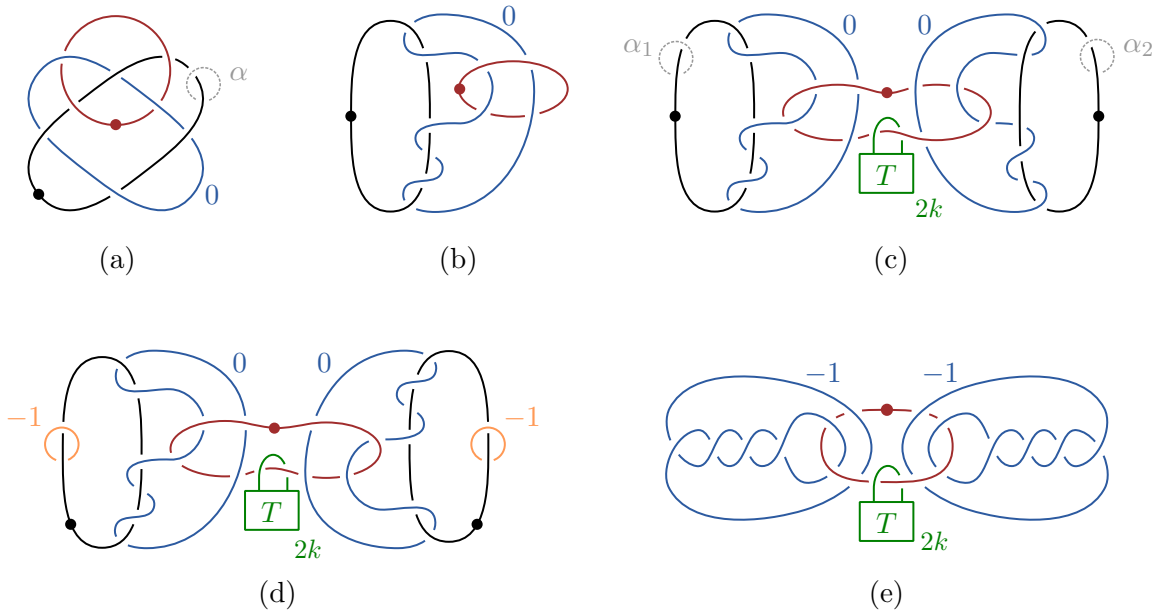


FIGURE 6.2

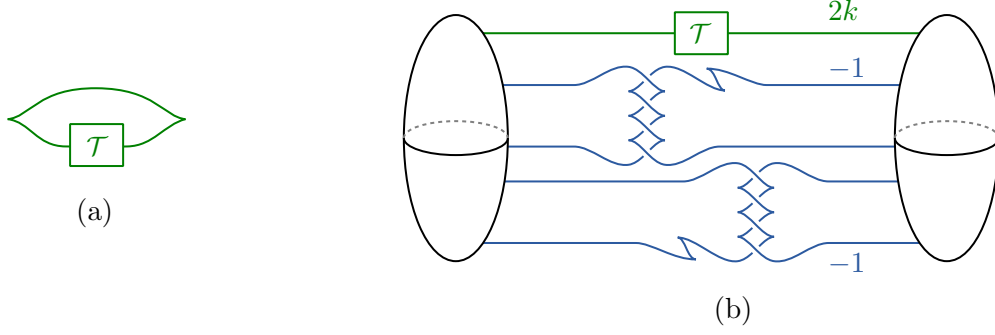


FIGURE 6.3. (a) Representing the Legendrian knot \mathcal{J} as the closure of a Legendrian tangle \mathcal{T} . (b) A Stein handle diagram for the 4-manifold X .

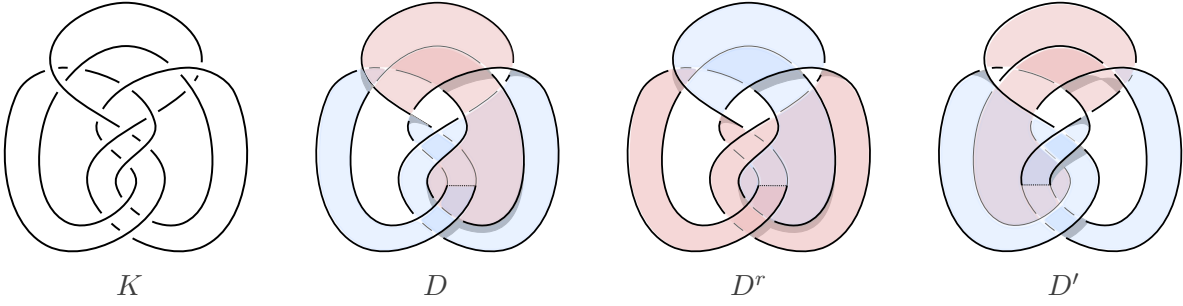
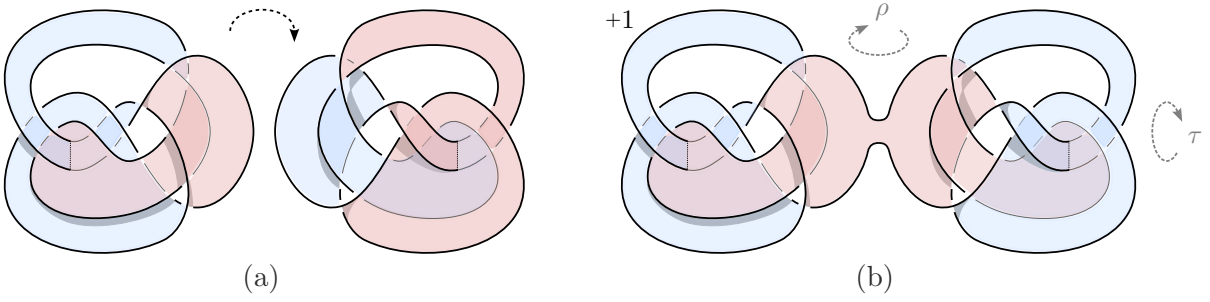
as an unknotted disk in a nonstandard the handle diagram of B^4 . Note that reversing the roles of the black and blue curves with a dot-zero swap gives a diagram for the exterior of D' . In turn, $W' = \Sigma_2(B^4, P_{J,k}(D'))$ is obtained by reversing the roles of the black and blue curves with a dot-zero swap. These branched covers W and W' are contractible 4-manifolds with identical boundary, hence are homeomorphic rel boundary [Fre82].

To see these 4-manifolds are not diffeomorphic rel boundary, consider attaching (-1) -framed 2-handles h_1 and h_2 to $\partial W = \partial W'$ along the two copies of the curve α in Figure 6.2(c). Since α bounds a smoothly embedded disk in $B^4 \setminus D'$ (as discussed in Example 2.5), it is straightforward to see that the enlarged 4-manifold $X' = W' \cup h_1 \cup h_2$ will contain a pair of smoothly embedded 2-spheres of square -1 . In contrast, consider the other enlarged 4-manifold $X = W \cup h_1 \cup h_2$ shown in Figure 6.2(d). We simplify this by a sequence of handleslides, two handle cancellations, and isotopy to obtain the alternative diagram in part (e). Now choose a Legendrian representative $\mathcal{J} \# \mathcal{J}^r$ of $J \# J^r$ with Thurston-Bennequin number $tb = 2k + 1$, and let \mathcal{T} be a Legendrian tangle whose closure as in Figure 6.3(a) is $\mathcal{J} \# \mathcal{J}^r$. (If necessary, we can ensure $\mathcal{J} \# \mathcal{J}^r$ has this form by performing Legendrian Reidemeister I moves.) Then X admits a Stein handle structure as depicted in Figure 6.3(b); see [Gom98] for background on Stein handle diagrams. Since X admits a Stein structure, it cannot contain any smoothly embedded 2-spheres of square -1 [LM97]. Hence we conclude that it is not diffeomorphic to X' , and thus W and W' are not diffeomorphic rel boundary.

To prove Theorem D, we leverage the fact that internal stabilization of knotted surfaces corresponds to external stabilization of their branched covers. In some cases, such as the one given below, exotically knotted surfaces may remain exotic after internal stabilization, yet the exotic branched covers of the original surfaces become diffeomorphic after external stabilization.

Proof of Theorem D. Let K denote the positron knot shown in Figure 6.4, and let D and D' denote the slice disks shown to its right. By Proposition 6.1, the branched double cover $\Sigma_2(B^4, D_{2,1})$ is diffeomorphic to $B_{+1}^4(D \natural D^r)$. The knot $K_{2,1}$ bounds a pair of genus-one surfaces $F, F' \subset B^4$ obtained by internally stabilizing the cabled disks $D_{2,1}, D'_{2,1} \subset B^4$, and the surfaces F and F' were shown to be exotically knotted in [Gut22].

We claim that the branched double covers $\Sigma_2(B^4, F)$ and $\Sigma_2(B^4, F')$ are diffeomorphic rel boundary. To that end, note that the branched double covers of $F = D_{2,1} \# T^2$ and $F' = D'_{2,1} \# T^2$ are diffeomorphic to $\Sigma_2(B^4, D_{2,1}) \# S^2 \times S^2$ and $\Sigma_2(B^4, D'_{2,1}) \# S^2 \times S^2$, respectively.

FIGURE 6.4. The positron knot K and slice disks that it bounds.FIGURE 6.5. Constructing $D \natural D^r$ and capping it off with the core of the 2-handle in $X = X_{+1}(K \# K^r)$.

By Proposition 6.1, the branched covers $\Sigma_2(B^4, D_{2,1})$ and $\Sigma_2(B^4, D'_{2,1})$ are diffeomorphic to $B_{+1}^4(D \natural D^r)$ and $B_{+1}^4(D' \natural (D')^r)$, so we turn our attention to these latter 4-manifolds.

The disk $D \natural D^r$ is illustrated in part (b) Figure 6.5 (ignoring the label $+1$ for the moment). Note that (up to reversing orientation), the disk $D' \natural (D')^r$ is obtained from $D \natural D^r$ by applying the involution τ of B^4 depicted by τ in Figure 6.5(b). Recall that $B_{+1}^4(D \natural D^r)$ can be constructed as follows: Let $X = X_{+1}(K \# K^r)$ denote the knot trace obtained by attaching a $(+1)$ -framed 2-handle to B^4 along $K \# K^r$, and let S and S' denote the smooth 2-spheres in X obtained by capping off D and D' , respectively, with the core of the 2-handle in X . Then $B_{+1}^4(D \natural D^r)$ and $B_{+1}^4(D' \natural (D')^r)$ are obtained by blowing down X along the $(+1)$ -framed 2-spheres S and S' , respectively.

To show that $B_{+1}^4(D \natural D^r)$ and $B_{+1}^4(D' \natural (D')^r)$ become diffeomorphic (rel boundary) after a single stabilization with $S^2 \times S^2$, it suffices to show that S and S' become isotopic (rel boundary) in $X \# S^2 \times S^2$. We prove this using arguments from [AKMR15], with our proof summarized in Figure 6.6: In part (a), we see the left half of $D \natural D^r$, viewed as a subset of $S \subset X \# S^2 \times S^2$. Passing from (a) to (b) uses the “key stable isotopy” from [AKMR15, Figure 5] (relying on the fact that S has simply connected complement in X). The subsurface of S shown in (b) is a disk in B^4 bounded by the unknot, hence is isotopic rel boundary to the alternative surface shown in (c). Reversing the “key stable isotopy”, we obtain part (d), at which point we have replaced the subset $D \natural D^r$ in S with $D' \natural D^r$. Having freed up the 2-handles corresponding to the $S^2 \times S^2$ -summand of $X \# S^2 \times S^2$, we can repeat this process and replace the subsurface D^r with $(D')^r$, thus producing an isotopy of $X \# S^2 \times S^2$ carrying S to S' . \square

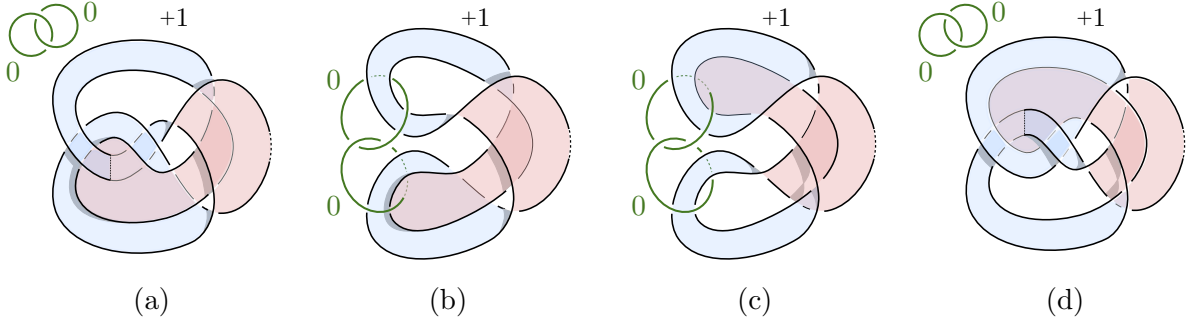


FIGURE 6.6. Applying the key stable isotopy from [AKMR15].

7. OBSTRUCTIONS FROM KHOVANOV HOMOLOGY

We close by proving Proposition E. For brevity, we assume background at the level of [BN05], and we refer the reader to [HS21, HKM⁺22, Hay23] for further background on calculations similar to the ones given here.

Proof. Let $K = m(9_{46})$ and consider the diagrams of K , $K_{2,1}$, and $\text{Wh}(K)$ shown in the top row of Figure 7.1. The bottom row of that figure depicts smoothings of these diagrams, where 0-resolved crossings are replaced with thin pink arcs (and 1-resolved crossings are unadorned). Note that the smoothings for $K_{2,1}$ and $\text{Wh}(K)$ are essentially obtained by “doubling” the smoothing for K , except where the additional crossings appear at the top of these diagrams. We obtain Khovanov chain elements by assigning each component of these smoothings the symbol x in the algebra $\mathcal{A} = \mathbb{F}_2\langle 1, x \rangle$. For each of these three chain elements, all 0-resolution arcs join distinct x -labeled components, so these chain elements are cycles [HS21, Proposition 2.1].

We claim that the latter two classes are mapped to $1 \in \mathbb{F}_2$ under the cobordism maps $\text{Kh}(D_{2,1})$ and $\text{Kh}(\text{Wh}(K))$. The first steps in these cobordisms are represented by the shaded bands in the diagrams of $K_{2,1}$ and $\text{Wh}(K)$; these indicate band moves which, after performing Reidemeister 1 moves, describe cobordisms from $K_{2,1}$ and $\text{Wh}(K)$ to the link $K_{2,0}$. (Note that these two cobordisms induce different orientations on the link $K_{2,0}$. This will not affect our calculation, so we ignore this detail.) Applying the induced map for these cobordisms (cf [HS21, Figure 11]), these classes are both carried to the class in $\text{Kh}(K_{2,0})$ shown in the top left of Figure 7.2. From here, these two cobordisms coincide with the doubled disk $D_{2,0}$, and the rest of the cobordism map calculation is summarized in Figures 7.2–7.3. In these figures, we use the label Δ to represent the split map (cf [HS21, Table 1]) and the labels $R1$, $R2_a$, and $R2_b$ to denote the chain maps depicted in the first, fifth, and sixth rows of [HS21, Table 2], respectively. The final step of each cobordism consists of four local minima capping off the four unknotted components on the top right side of Figure 7.3. Each circle in the associated chain element is x -labeled, so the associated cobordism map (cf [HS21, Table 1, second row]) maps the element to $1 \in \mathbb{F}_2$, as claimed.

Next we claim that these elements lie in the kernels of the maps $\text{Kh}(D'_{2,1})$ and $\text{Kh}(\text{Wh}(D'))$. These cobordisms begin with the same initial saddle cobordisms to $K_{2,0}$; as discussed above, the induced maps carry the elements in question to the class in $\text{Kh}(K_{2,0})$ depicted in the top left of Figure 7.2. From here, the cobordisms coincide with $D'_{2,0}$. This cobordism continues with the saddle move illustrated on the left side of Figure 7.4. At the chain level, this corresponds to a merge map (cf [HS21, Table 1, third row]) between two distinct x -labeled

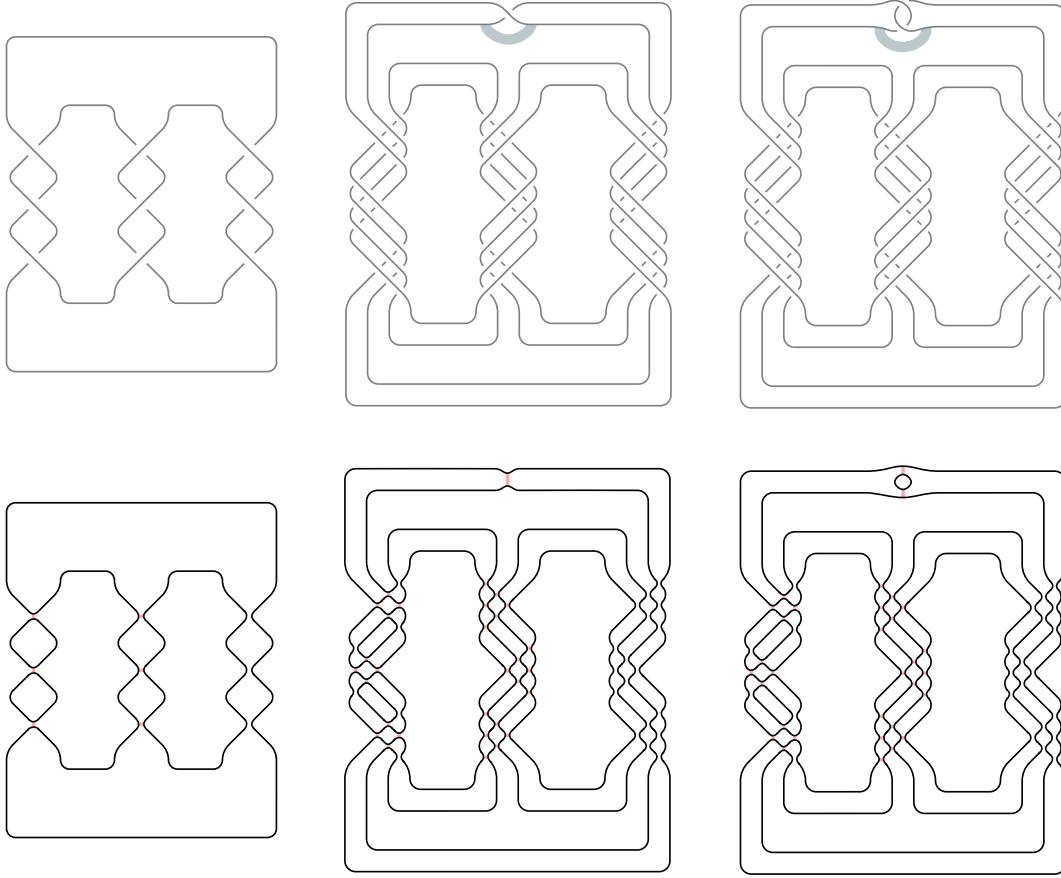


FIGURE 7.1. The top row presents diagrams for $K = m(9_{46})$, $\text{Wh}(K)$, and $K_{2,1}$. The bottom row depicts certain preferred smoothings of these diagrams.

components of the smoothing, hence vanishes. It follows that the element in question is mapped to $0 \in \mathbb{F}_2$.

Finally, we claim that the genus-one surfaces obtained by any internal stabilization of $D_{2,1}$ and $D'_{2,1}$ induce distinct maps on (reduced) Bar-Natan homology over $\mathbb{F}_2[U]$. The argument is analogous to the proof of [Hay23, Proposition 4.2], so we only outline it: First observe that the calculation establishing $\text{Kh}(D_{2,1}) \neq \text{Kh}(D'_{2,1})$ over \mathbb{F}_2 implies $\widetilde{\text{BN}}(D_{2,1}) \neq \widetilde{\text{BN}}(D'_{2,1})$ over $\mathbb{F}_2[U]$ (cf [Hay23, Proposition 4.1]). As a technical point, we note that working with the reduced theory $\widetilde{\text{BN}}$ requires puncturing our surfaces so that they are cobordisms between $K_{2,1}$ and the unknot. Next, consider the mirrored, time-reversed disks $-D_{2,1}$ and $-D'_{2,1}$. The duality of the cobordism maps under mirroring implies that the maps $\widetilde{\text{BN}}(-D_{2,1}), \widetilde{\text{BN}}(-D'_{2,1}) : \mathbb{F}_2[U] \rightarrow \widetilde{\text{BN}}(-K_{2,1})$ are distinct. Note that these maps are determined by the images of the generator $1 \in \mathbb{F}_2[U]$. By Euler characteristic considerations, these maps send $1 \in \mathbb{F}_2[U]$ to elements in bigrading $(h, q) = (0, 0)$. As verified by computer calculation (in [Sch21]) and depicted in Table 7.1, all nonzero elements in $\widetilde{\text{BN}}(-K_{2,1})$ with bigrading $(0, 0)$ survive multiplication by U . It follows that the difference $\widetilde{\text{BN}}(-D_{2,1})(1) - \widetilde{\text{BN}}(-D'_{2,1})(1)$ survives multiplication by U . Since internal stabilization has the effect of multiplying the cobordism maps by U ([LS22, Proposition 6.11]) the claim follows. \square

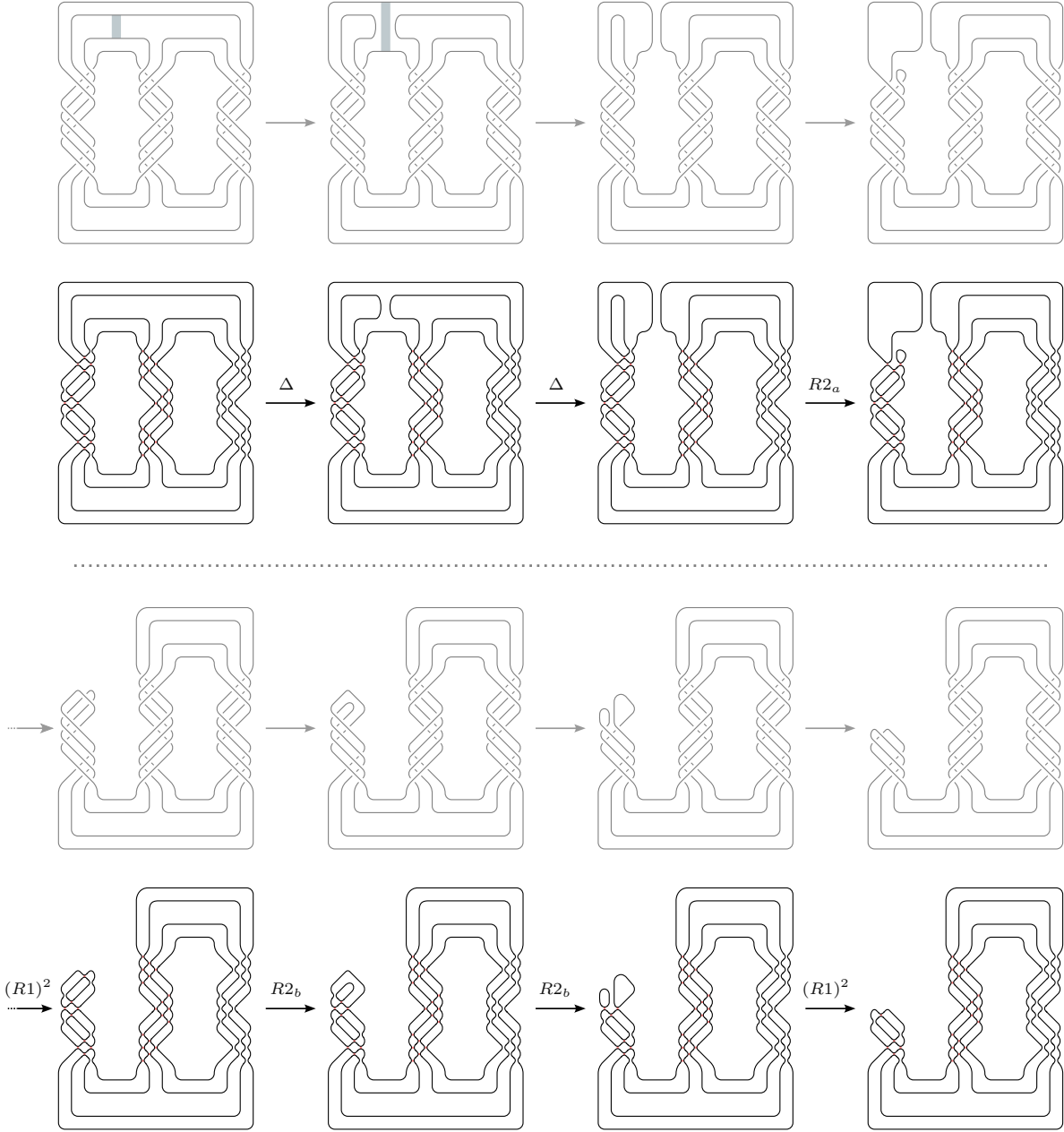


FIGURE 7.2. Calculating the initial steps of the cobordism map.

REFERENCES

- [AK80] Selman Akbulut and Robion Kirby, *Branched covers of surfaces in 4-manifolds*, Math. Ann. **252** (1979/80), no. 2, 111–131. MR 593626
- [Akb17] Selman Akbulut, *On infinite order corks*, Proceedings of the Gökova Geometry-Topology Conference 2016, Gökova Geometry/Topology Conference (GGT), Gökova, 2017, pp. 151–157. MR 3676087
- [AKMR15] Dave Auckly, Hee Jung Kim, Paul Melvin, and Daniel Ruberman, *Stable isotopy in four dimensions*, J. Lond. Math. Soc. (2) **91** (2015), no. 2, 439–463. MR 3355110

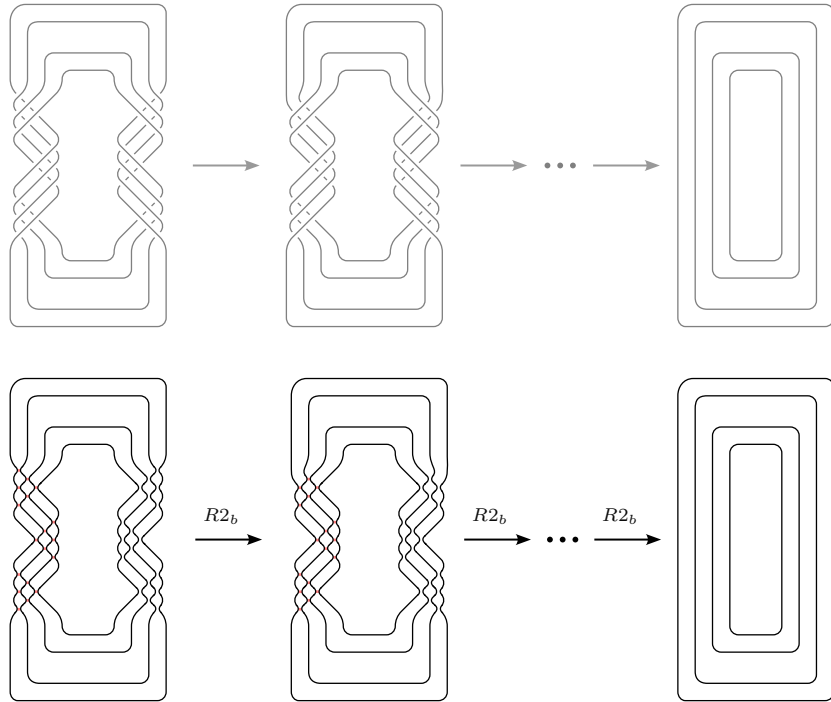
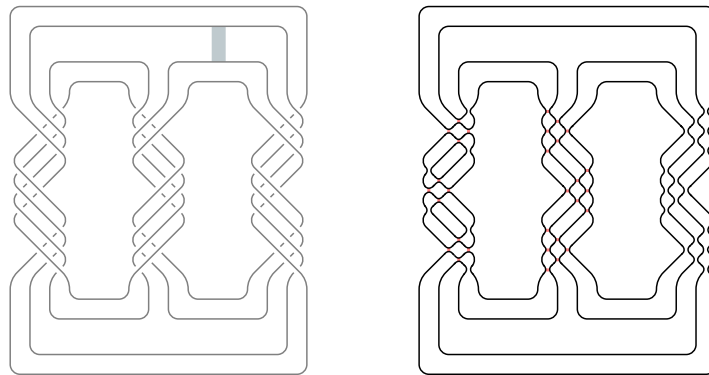


FIGURE 7.3. Calculating the final steps of the cobordism map.

FIGURE 7.4. The cobordism move for doubles of D' involve a saddle move along the band shown on the left. This saddle move merges two distinct circles in the smoothing on the right.

- [AR16] Selman Akbulut and Daniel Ruberman, *Absolutely exotic compact 4-manifolds*, Comment. Math. Helv. **91** (2016), no. 1, 1–19. MR 3471934
- [BN05] Dror Bar-Natan, *Khovanov's homology for tangles and cobordisms*, Geom. Topol. **9** (2005), 1443–1499. MR 2174270
- [BS16] R. İnanç Baykur and Nathan Sunukjian, *Knotted surfaces in 4-manifolds and stabilizations*, J. Topol. **9** (2016), no. 1, 215–231. MR 3465848
- [CDGW] Marc Culler, Nathan M. Dunfield, Matthias Goerner, and Jeffrey R. Weeks, *SnapPy, a computer program for studying the geometry and topology of 3-manifolds*, <http://snappy.computop.org>.
- [CP21a] Anthony Conway and Mark Powell, *Characterisation of homotopy ribbon discs*, Adv. Math. **391** (2021), Paper No. 107960, 29. MR 4300918

Page 1									
$h \backslash q$...	-3	-2	-1	0	1	2	3	4
4									1
2							1	1	
0					2	2	1		
-2				1	3	2			
-4			4	5	1				
-6		5	4	1					
-8		5	1						
-10									
\vdots									

Page 2									
$h \backslash q$...	-3	-2	-1	0	1	2	3	4
4									
2									
0					2				
-2									
-4				1					
-6									
-8									
-10									
\vdots									

TABLE 7.1. The first two pages of the reduced Bar-Natan–Lee–Turner spectral sequence for $(9_{46})_{2,1}$, shown for $h \geq -3$ and $q \geq -10$.

- [CP21b] ———, *Embedded surfaces with infinite cyclic knot group*, Geometry and Topology (2021).
- [DHM21] Irving Dai, Matthew Hedden, and Abhishek Mallick, *Corks, involutions, and Heegaard Floer homology*, arXiv:2002.02326 (2021).
- [FKV87] SM Finashin, M Kreck, and OY Viro, *Exotic knottings of surfaces in the 4-sphere*, Bulletin of the American Mathematical Society (New Series) **17** (1987), no. 2, 287–290.
- [Fox66] R. H. Fox, *Rolling*, Bull. Amer. Math. Soc. **72** (1966), 162–164. MR 184221
- [FQ90] Michael H. Freedman and Frank Quinn, *Topology of 4-manifolds*, Princeton Mathematical Series, vol. 39, Princeton University Press, Princeton, NJ, 1990. MR 1201584
- [Fre82] Michael Hartley Freedman, *The topology of four-dimensional manifolds*, J. Differential Geom. **17** (1982), no. 3, 357–453. MR 679066
- [FS97] Ronald Fintushel and Ronald J Stern, *Surfaces in 4-manifolds*, Mathematical Research Letters **4** (1997), no. 6, 907–914.
- [FS98] Ronald Fintushel and Ronald J. Stern, *Knots, links, and 4-manifolds*, Invent. Math. **134** (1998), no. 2, 363–400. MR 1650308
- [Glu62] Herman Gluck, *The embedding of two-spheres in the four-sphere*, Transactions of the American Mathematical Society **104** (1962), no. 2, 308–333.
- [Gom98] R. Gompf, *Handlebody construction of Stein surfaces*, Ann. of Math. (2) **148** (1998), no. 2, 619–693.
- [Gom17a] Robert E. Gompf, *Infinite order corks*, Geom. Topol. **21** (2017), no. 4, 2475–2484. MR 3654114
- [Gom17b] ———, *Infinite order corks via handle diagrams*, Algebr. Geom. Topol. **17** (2017), no. 5, 2863–2891. MR 3704246
- [GS99] Robert E. Gompf and András I. Stipsicz, *4-manifolds and Kirby calculus*, Graduate Studies in Mathematics, vol. 20, American Mathematical Society, Providence, RI, 1999. MR 1707327
- [Gut22] Gary Guth, *For exotic surfaces with boundary, one stabilization is not enough*, arXiv:2207.11847 (2022).
- [Hay23] Kyle Hayden, *An atomic approach to Wall-type stabilization problems*, arxiv:2302.10127 (2023).
- [Hed07] Matthew Hedden, *Knot floer homology of whitehead doubles*, Geometry & Topology **11** (2007), no. 4, 2277 – 2338.
- [HKK⁺21] Kyle Hayden, Alexandra Kjuchukova, Siddhi Krishna, Maggie Miller, Mark Powell, and Nathan Sunukjian, *Brunnian exotic surface links in the 4-ball*, Michigan Math. J. **arXiv:2106.13776** (2021).
- [HKM⁺22] Kyle Hayden, Seungwon Kim, Maggie Miller, JungHwan Park, and Isaac Sundberg, *Seifert surfaces in the 4-ball*, arXiv:2205.15283 (2022).
- [Hom14] Jennifer Hom, *Bordered Heegaard Floer homology and the tau-invariant of cable knots*, J. Topol. **7** (2014), no. 2, 287–326. MR 3217622
- [HS21] Kyle Hayden and Isaac Sundberg, *Khovanov homology and exotic surfaces in the 4-ball*, arXiv:2108.04810 (2021).
- [JM16] András Juhász and Marco Marengon, *Concordance maps in knot Floer homology*, Geom. Topol. **20** (2016), no. 6, 3623–3673. MR 3590358

- [JZ20] András Juhász and Ian Zemke, *Distinguishing slice disks using knot Floer homology*, Selecta Math. (N.S.) **26** (2020), no. 1, Paper No. 5, 18. MR 4045151
- [JZ21] András Juhász and Ian Zemke, *Stabilization distance bounds from link Floer homology*, arXiv:1810.09158 (2021).
- [Kir78] Rob Kirby, *Problems in low dimensional manifold theory*, Algebraic and geometric topology (Proc. Sympos. Pure Math., Stanford Univ., Stanford, Calif., 1976), Part 2, Proc. Sympos. Pure Math., XXXII, Amer. Math. Soc., Providence, R.I., 1978, pp. 273–312. MR 520548
- [Lev12] Adam Simon Levine, *Knot doubling operators and bordered Heegaard Floer homology*, J. Topol. **5** (2012), no. 3, 651–712. MR 2971610
- [LM97] P. Lisca and G. Matić, *Tight contact structures and Seiberg-Witten invariants*, Invent. Math. **129** (1997), no. 3, 509–525. MR 1465333
- [LOT18] Robert Lipshitz, Peter S. Ozsváth, and Dylan P. Thurston, *Bordered Heegaard Floer homology*, Mem. Amer. Math. Soc. **254** (2018), no. 1216, viii+279. MR 3827056
- [LS22] Robert Lipshitz and Sucharit Sarkar, *A mixed invariant of nonorientable surfaces in equivariant Khovanov homology*, Trans. Amer. Math. Soc. **375** (2022), no. 12, 8807–8849. MR 4504654
- [LZ22] Lukas Lewark and Claudius Zibrowius, *Rasmussen invariants of whitehead doubles and other satellites*, arXiv:2208.13612 (2022).
- [OS04a] Peter Ozsváth and Zoltán Szabó, *Holomorphic disks and genus bounds*, Geom. Topol. **8** (2004), 311–334. MR 2023281
- [OS04b] ———, *Holomorphic disks and knot invariants*, Adv. Math. **186** (2004), no. 1, 58–116. MR 2065507
- [OSS17] Peter Ozsváth, András I. Stipsicz, and Zoltán Szabó, *Concordance homomorphisms from knot Floer homology*, Adv. Math. **315** (2017), 366–426. MR 3667589
- [PW21] Ina Petkova and Biji Wong, *Twisted Mazur pattern satellite knots and bordered Floer theory*, Michigan Mathematical Journal **1** (2021), no. 1, 1–50.
- [Ras03] Jacob Andrew Rasmussen, *Floer homology and knot complements*, ProQuest LLC, Ann Arbor, MI, 2003, Thesis (Ph.D.)—Harvard University. MR 2704683
- [Rot95] Joseph J. Rotman, *An introduction to the theory of groups*, fourth ed., Graduate Texts in Mathematics, vol. 148, Springer-Verlag, New York, 1995. MR 1307623
- [Rub90] Daniel Ruberman, *Seifert surfaces of knots in S^4* , Pacific Journal of Mathematics **145** (1990), 97–116.
- [Sar15] Sucharit Sarkar, *Moving basepoints and the induced automorphisms of link Floer homology*, Algebr. Geom. Topol. **15** (2015), no. 5, 2479–2515. MR 3426686
- [Sch21] Dirk Schütz, *KnotJob*, Available at <http://www.maths.dur.ac.uk/~dma0ds/knotjob.html>, 2021.
- [Shi71] Yaichi Shinohara, *Higher dimensional knots in tubes*, Trans. Amer. Math. Soc. **161** (1971), 35–49. MR 287559
- [Sza] Zoltán Szabó, *Knot Floer homology calculator*, <https://web.math.princeton.edu/~szabo/HFKcalc.html>.
- [Tra82] Bruce Trace, *On attaching 3-handles to a 1-connected 4-manifold*, Pacific J. Math. **99** (1982), no. 1, 175–181. MR 651494
- [Zem16] Ian Zemke, *Quasi-stabilization and basepoint moving maps in link floer homology*, arXiv: Geometric Topology (2016).
- [Zem18] Ian Zemke, *Link cobordisms and functoriality in link Floer homology*, Journal of Topology **12** (2018), no. 1, 94–220.
- [Zib22] Claudius Zibrowius, *Heegaard floer multicurves of double tangles*, arXiv preprint arXiv:2212.08501 (2022).

DEPARTMENT OF MATHEMATICS, STANFORD UNIVERSITY, STANFORD, CA 94305 USA

Email address: `gmguth@stanford.edu`

DEPARTMENT OF MATHEMATICS AND COMPUTER SCIENCE, RUTGERS UNIVERSITY, NEWARK, NJ 07102, USA

Email address: `kyle.hayden@rutgers.edu`

MATHEMATICAL INSTITUTE, UNIVERSITY OF OXFORD, ANDREW WILES BUILDING, RADCLIFFE OBSERVATORY QUARTERS, WOODSTOCK ROAD, OXFORD, OX2 6GG, UNITED KINGDOM

Email address: `sungkyung3838@gmail.com`

DEPARTMENT OF MATHEMATICAL SCIENCES, KAIST, DAEJEON 34141, REPUBLIC OF KOREA

Email address: `jungpark0817@kaist.ac.kr`